



NTNU – Trondheim
Norwegian University of
Science and Technology

Aerodynamic Development of DNV GL Fuel Fighter

Towards Shell Eco Marathon 2015

Myselie Nguyen

Master of Energy and Environmental Engineering

Submission date: June 2015

Supervisor: James Dawson, EPT

Norwegian University of Science and Technology
Department of Energy and Process Engineering

EPT-M-2014-61

MASTER THESIS

Name: Myselie Nguyen

Spring 2015

*Aerodynamic Development of the DNV GL fuel fighter***Background and objective**

This project supports the larger initiative of student run NTNU entrance into the Shell Eco Marathon. The aim is to design a car to travel as far as possible for the lowest amount of fuel consumption. There is some interest in optimising the aerodynamics performance of the car using CFD which requires proper benchmarking and validation. The objective of the project is to carry out the first steps needed to document the optimise the aerodynamics to minimise drag.

The student will perform the following tasks:

- Understand and identify the different sources that contribute to total drag on a vehicle.
- Design and perform wind tunnel experiments to measure the drag of a scale model of the the 2015 entry.
- Carry out CFD and test new car design

Within 14 days of receiving the written text on the master thesis, the candidate shall submit a research plan for his project to the department.

When the thesis is evaluated, emphasis is put on processing of the results, and that they are presented in tabular and/or graphic form in a clear manner, and that they are analyzed carefully.

The thesis should be formulated as a research report with summary both in English and Norwegian, conclusion, literature references, table of contents etc. During the preparation of the text, the candidate should make an effort to produce a well-structured and easily readable report. In order to ease the evaluation of the thesis, it is important that the cross-references are correct. In the making of the report, strong emphasis should be placed on both a thorough discussion of the results and an orderly presentation.

The candidate is requested to initiate and keep close contact with his/her academic supervisor(s) throughout the working period. The candidate must follow the rules and regulations of NTNU as well as passive directions given by the Department of Energy and Process Engineering.

Risk assessment of the candidate's work shall be carried out according to the department's procedures. The risk assessment must be documented and included as part of the final report.

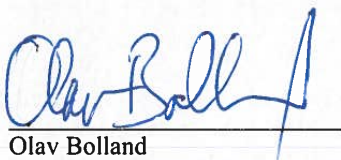
Events related to the candidate's work adversely affecting the health, safety or security, must be documented and included as part of the final report. If the documentation on risk assessment represents a large number of pages, the full version is to be submitted electronically to the supervisor and an excerpt is included in the report.

Pursuant to "Regulations concerning the supplementary provisions to the technology study program/Master of Science" at NTNU §20, the Department reserves the permission to utilize all the results and data for teaching and research purposes as well as in future publications.

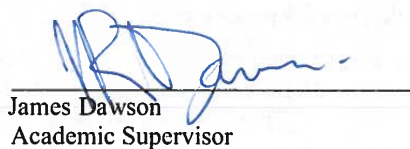
The final report is to be submitted digitally in DAIM. An executive summary of the thesis including title, student's name, supervisor's name, year, department name, and NTNU's logo and name, shall be submitted to the department as a separate pdf file. Based on an agreement with the supervisor, the final report and other material and documents may be given to the supervisor in digital format.

- Work to be done in lab (Water power lab, Fluids engineering lab, Thermal engineering lab)
 Field work

Department of Energy and Process Engineering, 14. January 2015



Olav Bolland
Department Head



James Dawson
Academic Supervisor

Research Advisor:

Abstract

Shell Eco Marathon (SEM) is an international engineering competition for university students. The aim of the competitions is to build a vehicle that achieves the highest possible energy efficiency. DNV GL Fuel Fighter is NTNU's contribution to SEM 2015. This year team consist of 25 student from different studies, where everyone has their area of expertise in the project.

The team decided to develop a new Urban Concept vehicle that has a totally different design compared to previous NTNU Urban Concepts. This text is going to be focusing on the aerodynamic aspect of developing the new Urban Concept. The team used the production development methodology from the department of Design Engineering and Materials (IPM) from the Norwegian University of Science and Technology (NTNU). The IPM methodology has four different phases, where the aerodynamic aspect was in all phases.

There were two design concepts that were of interest, and which got further aerodynamic analysis by intuition, CFD (Computational Fluid Dynamics) and wind tunnel testing in order to minimize the drag coefficient. Aerodynamics of vehicles are more than just minimizing the drag coefficient, but it was only time to go through that aerodynamic aspect of developing a vehicle.

Concept 1 had a drag coefficient of 0.32 and Concept 2 had a drag coefficient of 0.27, which were good compared to a normal passenger vehicle that has a drag coefficient between 0.30-0.45. The chosen concept was Concept 2, not only because it has lower drag coefficient, but also producing Concept 2 was much easier than Concept 1.

During SEM the Urban Concept didn't get any approved attempts, because of some problems with the hydrogen leakage from the fuel cells. However, the team was a runner up on the "design off track award", which was also the team's objective.

Sammendrag

Shell Eco Marathon (SEM) er en internasjonal ingeniørkonkurranse for studenter. Målet er å bygge en bil som oppnår høyest mulig energieffektivitet. DNV GL Fuel Fighter er NTNUs bidrag til SEM 2015. Årets team består av 25 studenter fra forskjellige studier, der alle har sitt område av ekspertise i prosjektet.

Teamet bestemte seg for å utvikle en ny Urban Concept bil som har en helt annerledes design i forhold til tidligere NTNU-biler i Urban Concept klassen. Denne teksten kommer til å fokusere på den aerodynamiske aspektet av å utvikle den nye Urban Concept. Teamet brukte IPMs sin produksjon og produktutviklingsmetodikk, som har fire forskjellige faser.

Det var to designkonsept som var av interesse, og fikk ytterligere aerodynamisk analyse vha. intuisjon, CFD (Computational Fluid Dynamics) og vindtunneltesting for å minimere luftmotstandskoeffisienten. Aerodynamisk teori om biler handler om mer enn bare å minimere luftmotstand, men dette var det eneste som det var tid til.

Concept 1 hadde en luftmotstandskoeffisient på 0,32 og Concept 2 hadde en luftmotstandskoeffisient på 0,27, noe som var bra i forhold til en normal personbil som har en luftmotstandskoeffisient mellom 0.30 - 0.45. Det valgte konseptet var Concept 2, ikke bare fordi den har lavere luftmotstand, men den var også lettere å produsere i forhold til Concept 1.

Under SEM Urban Concept ikke fikk noe godkjent forsøk, på grunn av noen problemer med hydrogen lekkasje fra brenselceller. Men teamet var på andre plass på "offtrackdesign prisen, som også var teamets målsetning.

Preface and Acknowledgement

My name is Myselie Nguyen and this text is my master thesis for the degree in Master of Science and Technology in Energy and Environmental Engineering program of the Norwegian University of Science and Technology (NTNU).

I was a part of a project called DNV GL Fuel Fighter, where the main goal was to develop a fuel efficient vehicle to compete in the international competition Shell Eco Marathon (SEM). The project was a cooperation project between 25 students from different study programs, where seven of the team members were also writing their theses in the project. My main task was the aerodynamic aspects of the vehicle, as well as being the project manager.

My supervisor for the aerodynamic development is professor James Dawson from the department of Energy, Process Engineering and Fluid dynamics. The department of Engineering Design and Materials at NTNU, with associate professor Knut Einar Aasland, is the main supervisor of the over all project. I would like to start by acknowledging both my professors for guidance and giving the opportunity to work on this very interesting project.

Thanks to the team members in the DNV GL Fuel Fighter team for welcoming me as a project manager and aerodynamics engineer. The team has dedicated a lot of time to the project and has made this a memorable time. A special thanks to Vegard Dahle and Bård Sve Wallentinsen for proofreading this text.

At last, I would also like to thank my parents for all the guidance and their leading by example. Mom, your tenacity by even studying in old age has inspired me and Dad you have been to all my football matches, which shaped me to be the person I am today. You have both always inspired me to be well educated, so by this I will dedicate this text for you, my Mom and Dad.

Trondheim 10th of June 2014
Myselie Nguyen



Contents

List of Figures	x
List of Tables	xii
1 Introduction	1
1.1 Shell Eco Marathon	1
1.2 DNV GL Fuel Fighter	3
1.3 Fuel Consumption	7
1.4 IPM methodology	8
1.5 How to read the text	10
2 The theory of vehicle design	13
2.1 The energy and fuel consumption	13
2.2 Aerodynamic Vehicle Design	16
2.3 Tools of aerodynamic analysis	18
2.3.1 CFD	20
2.3.2 The wind tunnel	23
3 The vehicle design approach	27
3.1 The design concepts	27
3.2 The intuitive aerodynamic analysis	28
3.3 The CFD set up	31
3.3.1 Discussion and comparison of the CFD results	34
3.4 Validation by Wind tunnel testing	37
4 The new Urban Concept	41
4.1 Phase 4 - Structure and form	41
4.2 Phase 5 - Production Preparation	42
4.3 The end product result	45
5 Further work - Advice to next year's team	47
References	51

Appendices	
A The SEM requirements	55
B User requirements	57
C The Buckingham Pi Dimension analyse	61
D The tyre properties of the Old Urban Concept	66
E The calibration of the Beam scale	68
F The calibration of the Pitot tube	70
G Urban Concept 1 Fluent set up script	71
H Urban Concept 2 Fluent set up script	79
I The wind tunnel data result	87
J The morphology table	89

List of Figures

1.1	Examples of SEM's Prototype [1, 2, 3]	2
1.2	Examples of SEM's Urban Concept [4, 5, 6]	2
1.3	The 2015 track at Ahoy!, Rotterdam, Netherlands	3
1.4	The 2015 NTNU team - DNV GL Fuel Fighter	5
1.5	The team's structure	6
1.6	A flow chart of the fuel and energy efficiency dependency for a vehicle	7
1.7	An illustration of the five phases of the IPM-methodology	8
1.8	Examples of the concept sketches	9
2.1	An illusion of the forces action on the vehicle [7]	14
2.2	An illusion of the cross sectional area A [7]	15
2.3	An illusion of the wind velocities vectors [7]	15
2.4	An illustration of the two flow separation types	16
2.5	Scibor-Rylski ideal shape based on NACA2415 and NACA0030 [8]	17
2.6	Streamline around a sphere and an airfoil, and their respective drag coefficients [9]	18
2.7	The difference in relative motion between road driving and CFD and wind tunnel testing [7]	20
2.8	The different mesh done on a sphere	21
2.9	A brief hierarchy of the turbulence model	23
2.10	An illustration of the two wind tunnel types [7]	24
3.1	The two previous NTNU Urban Concepts	27
3.2	Concept 1	28
3.3	Concept 2	28
3.4	Aerodynamic modification of concept 1	28
3.5	The figures show the notchback and hatchback configuration, for comparison	29
3.6	A graphical display of the relationship between the normalised drag coefficient and the effective rear end slope [8]	30
3.7	The Rumpler Limousine of 1921 [10]	30
3.8	A simplified CAD-model of both concepts	31

3.9	The computational domain, where it got cut in the longitudinal direction the vehicle	32
3.10	The refined mesh area, with zoomed mesh to show the inflation mesh on the surface of the vehicle and the ground	33
3.11	Total pressure contours on the vehicles at 30km/h	36
3.12	The streamlines of Concept 1	36
3.13	The streamlines of Concept 2	37
3.14	Pictures of the scaled model	38
3.15	Reynolds number vs drag coefficient	40
4.1	Detailed CAD figures from Siemens NX 9.0	41
4.2	The negative molds of the vehicle in 6 pieces for production	43
4.3	A figure of the carbon fiber weaves	44
4.4	The monocoque with a smooth surface, before being foiled red	44
4.5	Pictures of the end result	45
5.1	The streamline of the new Urban Concept	48
5.2	The fuel cells and motor's ventilation system	48

List of Tables

1.1	Table of the core team members	4
1.2	A summary table of the reports in DNV GL Fuel Fighter project	10
3.1	Boundary conditions and assumptions for the simulations of the two concepts	33
3.2	The simulation results with the according amount of mesh elements	35
3.3	The wind tunnel results	39
4.1	Overview of the vehicle dimensions	42

Chapter 1

Introduction

The first section, 1.1, shall explain more about the Shell Eco Marathon competition. Section 1.2 is about the NTNU team DNV GL Fuel Fighter and the results it got in SEM. A summary of the fuel aspects are shown in section 1.3. Section 1.4 shall go through the phases of the IPM methodology. Section 1.5 outlines the texts related to this team project.

1.1 Shell Eco Marathon

Shell Eco-marathon (SEM) is an annual international student engineering competition, which takes place in Asia, America and in Europe. The main goal is to develop a vehicle that is as fuel or energy efficient as possible. Additionally there are off-track awards, such as the Design Award, Safety Award, Technical Innovations Award and Communication Award. SEM is divided into two vehicle classes; the Prototype class and the Urban Concept class. The main difference between the two classes is the design requirements.

In the **Prototype** class the sole aim is to design a vehicle that minimizes fuel consumption. So the vehicles usually have very low weight and very small frontal area, to reduce the friction and aerodynamic drag. This results in a vehicle with only the absolute minimum of functionality, which usually does not look like a passenger vehicle. The SEM rules state that safety for the contestant is the most important aspect of the design. Therefore it is mandatory to have a seat belt, a mirror and a horn, and the driver is not allowed to lay down on the stomach with the head first position. It is allowed to be lying on the back, but the driver has to have a visibility of 90° of each side of the longitudinal axis of the vehicle. Figure 1.1 shows examples of SEM prototype vehicles.



Figure 1.1: Examples of SEM's Prototype [1, 2, 3]

In the **Urban Concept** class, the vehicle designs have more restrictions. For instance, vehicles need to have four wheels, lights, wind shield wipers and a luggage room. Therefore the design of the Urban Concept is closer to that of a normal passenger car, although it is only required to have one seat. The rules state that the maximum weight of the vehicle is 225 kg, which is also much lighter than a passenger car. Figure 1.2 shows examples of SEM Urban Concept designs.



Figure 1.2: Examples of SEM's Urban Concept [4, 5, 6]

Within each of the two vehicle classes there is also a division into five different fuel alternative classes:

- Electrical battery
- Petrol/Gasoline
- Diesel
- Hydrogen Fuel Cell
- Alternative Fuel (examples: ethanol, bio-fuel, CNG)

The competition of SEM Europe 2015 was held at Ahoy!, Rotterdam, Netherlands from the 18th to the 24th of May. It was the third and the last time the competition was held at Ahoy!. Next year (in 2016) SEM Europe will be held in London. The track in 2015 is shown in figure 1.3. The rules state that both vehicle classes have

to drive 10 laps of 1 626 meters within 39 minutes, with the additional requirement that the Urban Concept stops once every lap, to simulate traffic lights. This gives a required average speed of 25 km/h. Each team will be limited to four official attempts: the best result will be retained for the final classification. More rules can be found on Shell Eco Marathon's homepage [11].

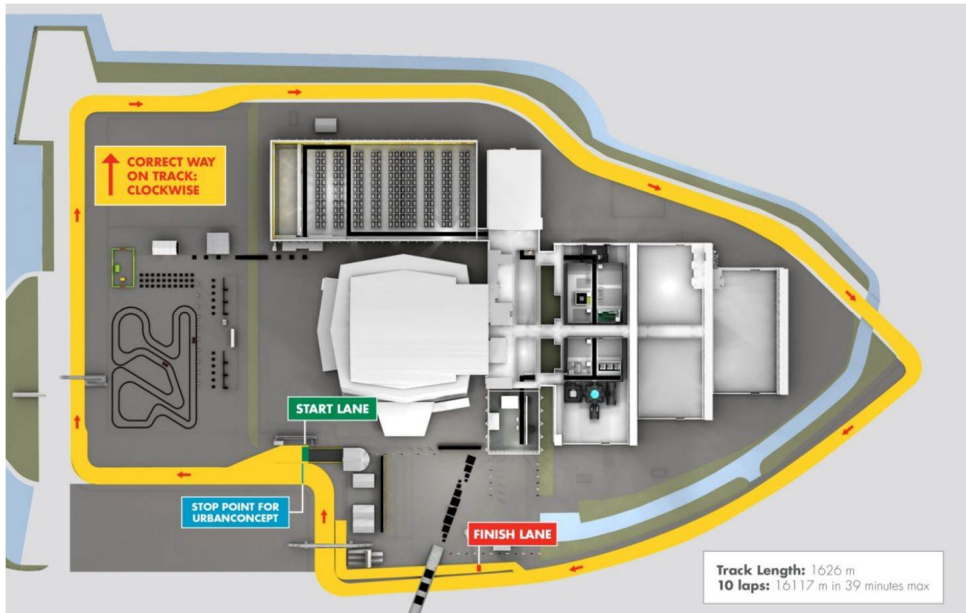


Figure 1.3: The 2015 track at Ahoy!, Rotterdam, Netherlands

1.2 DNV GL Fuel Fighter

NTNU has been a part of SEM every year since 2009. Throughout the years the NTNU team has built two different Urban Concepts, in 2009 and 2012, and a Prototype in 2014. In the years between building new vehicles, different mechanical and electrical modifications were carried out.

DNV GL Fuel Fighter is NTNU's 2015-team. It started in August 2014 with seven master students from different engineering disciplines. The master students have their specific task with their own supervisor in the project, see table 1.1. These seven master students will be referred as the **core team** throughout this text.

Table 1.1: Table of the core team members

Name	Master thesis in the project	Supervisor
Myselie Nguyen	Aerodynamics engineer, studying the aerodynamics aspects of the car	James Dawson from EPT NTNU
Hossein Neizan Hosseini	System manager, studying the reliability of the car	Cecilia Haskins from IPK NTNU
Benjamin Halsøy	Mechanical engineer, Development and Production of the cars	Knut Einar Aasland from IPM NTNU
Magnus Buodd	Mechanical engineer, Development and Production of the cars	Knut Einar Aasland from IPM NTNU
Yoann Dolle	Mechanical engineer, Development and Production of the cars	Knut Einar Aasland from IPM NTNU
Ole Bauck	Cybernetics engineer, designing a fuel efficient motor controller	Amund Skavhaug from ITK NTNU
Vebjørn Røed Myklebust	Cybernetics engineer, designing a radio communication to the car	Amund Skavhaug from ITK NTNU

The table 1.1 shows that the students are from different faculties. The main supervisor for the project is Knut Einar Aasland from the faculty of Engineering Design and Materials (IPM). Even though Aasland is the main supervisor of the project, he gave free rein for all the decision to the students. This also included the responsibility of getting sponsors for equipment and other funding. The project is a non-profit organisation, and it is based on the volunteer work of the students.



Figure 1.4: The 2015 NTNU team - DNV GL Fuel Fighter

The core team decided to make vast innovations in both vehicle classes for SEM2015, with a brand new Urban Concept in the hydrogen class, and a modified Prototype from 2014 in the electrical battery class. The team had only eight months until the competition. Due to the ambitious plan, the core team needed to expand, and therefore spent the first month recruiting team members. After the recruitment the team ended up with 25 students from different disciplines, five non-technical (PR, photographer, etc), and the rest of the team engineering students from different disciplines and nationalities. Figure 1.4 shows the team picture after the revealing the new Urban Concept, with the Sustainability Chief Officer from DNV GL, our main sponsor, and our ambassador Nina Jensen, the President of WWF.

The team were divided into six work areas, where the core team got, in addition to their respective Master's Theses, a management job within their area. For example the Cybernetics engineers, listed above as part of the core team, became managers for the electrical team, and so on. Meanwhile, Myselie Nguyen (the text author), the aerodynamic engineer, became the team's project manager. The team's organizational structure corresponds to figure 1.5. The arrows in figure 1.5 represent that everyone in the team have to help each other from development to building, not merely focusing on their own task or thesis.

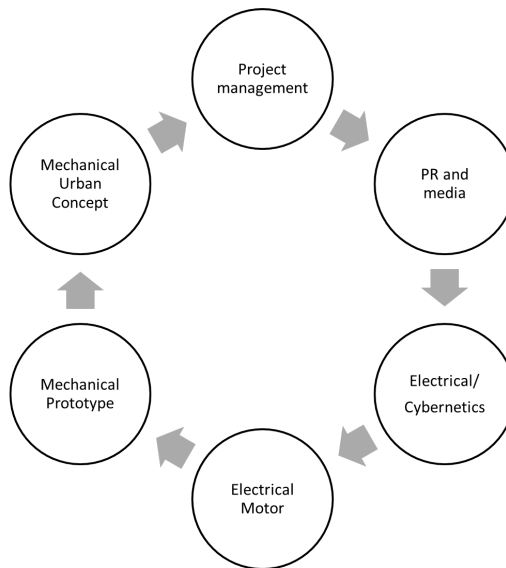


Figure 1.5: The team's structure

- The project manager including the system manager and the project manager. The project manager has the main responsibility of the planning, economy, execution and closing of the project.
- The PR-team were spreading the information of the project to the public by the press and social media.
- The electrical team were developing the whole electrical system, including GPS, lights and horns, etc., on both vehicles.
- The electrical transmission from the engine to the wheels were the same for both vehicles. This is an area which, if handled well, can save a lot of energy consumption, and therefore it was assigned as a separate field, as shown in figure 1.5.
- The Prototype from 2014 came in 7th place in the electrical battery class. The Prototype has a really good aerodynamic design, and has the potential to win. Therefore is this an own working area. The mechanical work were the vehicle losing weight and changing the transmission system from the engine to the wheel.
- The Urban Concept team were designing and developing the new Urban Concept.

1.3 Fuel Consumption

The public interest in SEM and its focus on fuel efficiency has increased in recent years. This probably has two main reasons; first, the classical and the most common vehicle fuel of SEM is gasoline, a fuel which gives emission that affect the climate. Second, the gasoline prizes gets more expensive over the years.

A vehicle's fuel consumption depends on the efficiency of the transmission system between the engine and the fuel, the efficiency of the engine, and the power required to overcome the resistance of the motion. Equation 1.1 shows the derivation of the power required to overcome the resistance of the motion

$$\text{power} = \text{total resistance force} * \text{speed} \quad (1.1)$$

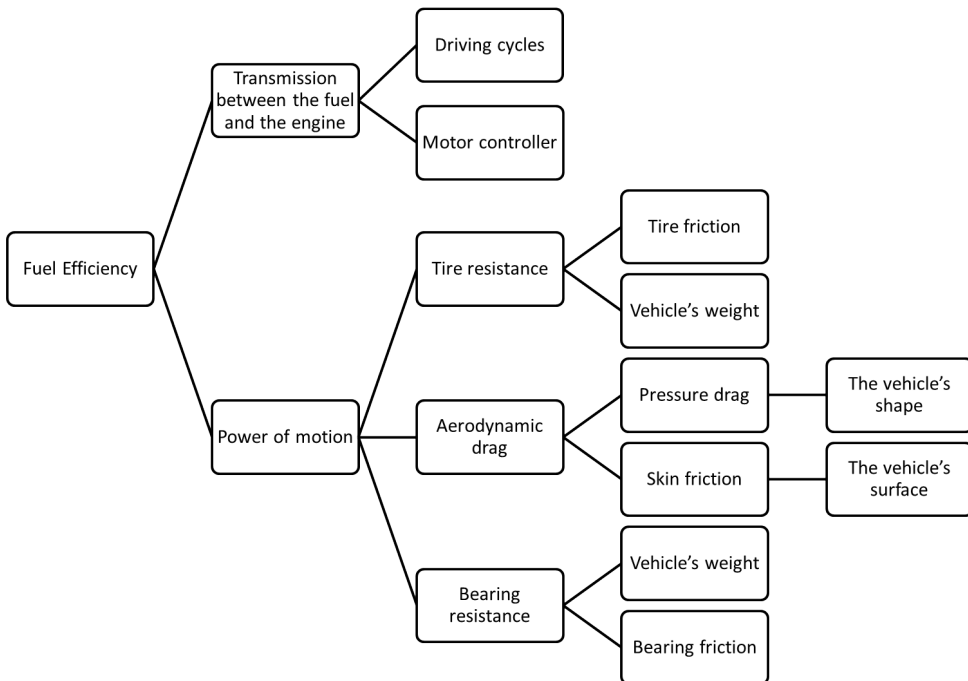


Figure 1.6: A flow chart of the fuel and energy efficiency dependency for a vehicle

In equation 1.1 the total resistance force is mainly the sum of aerodynamic drag, bearing resistance and tire rolling resistance. The aerodynamic drag depends on the shape of the vehicle and the surface roughness of the vehicle. The tire rolling

resistance depends on both the weight of the car and the tire resistance. Finally, the bearing resistance depends on both the weight of the car and the resistance of the bearing. Figure 1.6 shows the flow chart of the dependencies for fuel and energy efficiency for a vehicle. For developing a fuel efficient vehicle, all the properties at the end of the flow chart has to be considered. This text will go through the flow chart of the aerodynamic drag.

1.4 IPM methodology

The department of IPM at NTNU has developed a methodology for producing a new product, called the **IPM-methodology**. The team used this methodology to monitor the progress of the project. The IPM-methodology is divided into five phases, which are shown in figure 1.7.

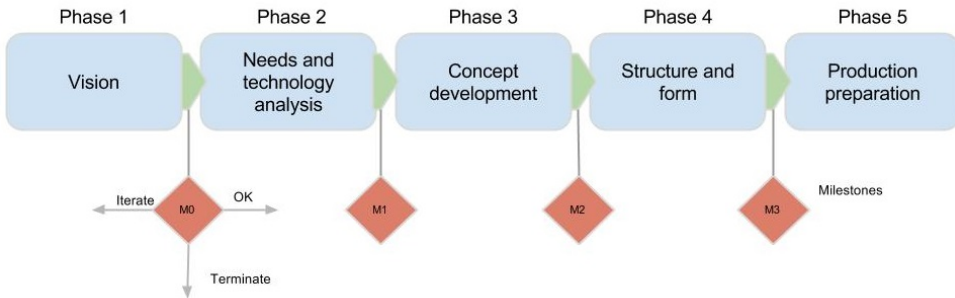


Figure 1.7: An illustration of the five phases of the IPM-methodology

In figure 1.7 the model contains milestones, which indicate the end of a phase. When reaching a milestone the team must evaluate the phase; if the phase is not finished in a satisfactory way, the team has to take a step back and re-evaluate the work. If the requirements of the phase are satisfied, the team takes a step forward. Even though illustration and description so far has indicated a linear product development process the reality is far from linear. The team had to jump back and and forth between phases as new information appears.

Phase 1 - Vision & Mission To systematically develop a new product it is important to have a clear vision and mission for the project. This helps the team gain a common understanding of the goal for the project. For the development of the Urban Concept, the vision, and mission were the following:

Vision: "Create a buzz around the project and perform on top level on Shell Eco-marathon"

Mission: "Making a a new Urban Concept that has the potential to win the Design Award"

Phase 2 - Needs The needs of four stakeholders, have to be fulfilled. These are the needs of; 1. the driver, 2. The SEM administration, represented by the SEM rules, 3. The team 4. The sponsors. Appendix B gives a list of the different user demands and appendix A has the list of SEM requirements. Also the needs of making a fuel efficient vehicle had to be analyzed, which is shown in figure 1.6.

Phase 3 - Concept development

Within this phase of concept development, there were also two other steps. It started with blank sheets and sketching the different vehicle designs, and combining the wanted feature of the designs, as figure 1.8 shows. Two concept were chosen for further aerodynamic analyse by intuition, CFD (Computational Fluid Dynamic) analysis and wind tunnel testing. More about the aerodynamic development in phase 3 in chapter 3.

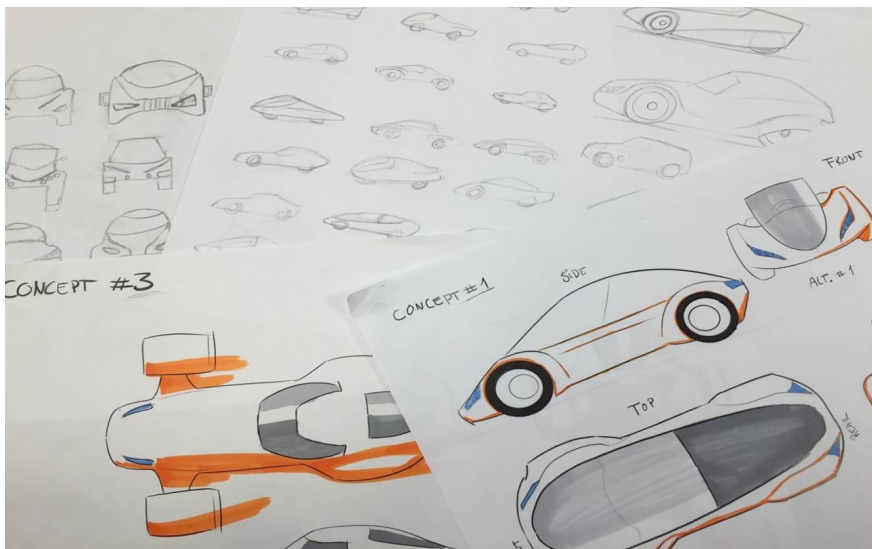


Figure 1.8: Examples of the concept sketches

Phase 4 - Structure and form, and Phase 5 - Preparing for Production

To analyse the structure and form a detailed CAD model needed to be modelled. This gave a clearer visualization of the concept. Also strength calculations was needed, to have the material choices, shapes and the dimensions ready, to prepare for production. A plan of the production process and the needed help are clarified later in the text, in chapter 4.

1.5 How to read the text

This text will be focusing solely on the aerodynamic aspects of developing the new Urban Concept vehicle. Table 1.2 shows the other reports from the project, that are complementary to this text for a full understanding of the project. The first report in table 1.2 is the overall report for the project, including the project management, PR, graphical design, etc.

Table 1.2: A summary table of the reports in DNV GL Fuel Fighter project

The report's name	Focus area	Supervisor
Master thesis: DNV GL Fuel Fighter towards Shell Eco Marathon 2015 [12]	The overall report of the project and the team, from designing, production and management	Knut Einar Aasland from IPM NTNU
Master thesis: Reliability Systems Engineering For Shell Eco-Marathon Competition [13]	System manager, finding the reliability of the car	Cecilia Haskins from IPK NTNU
Master thesis: Hardware and software design for the DNV GL Fuel Fighter vehicles [14]	Cybernetics engineer, designing a fuel efficient motor controller and radio communication of the cars and analysing the driving cycle	Amund Skavhaug from ITK NTNU
Driver Interface for Shell Eco Marathon Vehicle [15]	Cybernetics engineer, designing the electrical interface with the driver, having back screen sensor and etc.	Amund Skavhaug from ITK NTNU
Bachelor thesis: The rear suspension, gear and motor mount for the DNV GL FuelFighter Urban concept car 2015 [16]	Back wheel suspension	Bård Brøndstad HiST

The first chapter gave an introduction to the whole text. Chapter 2 shall go through the theory of aerodynamically developing a vehicle. Where the aerodynamic aspect of phase 3 for the IPM methodology are shown in chapter 3. The two last phases for the IPM methodology are shown in chapter 4.

Chapter 2

The theory of vehicle design

The theory for aerodynamics design is the same for SEM vehicles as it is for passenger vehicles. The aerodynamic design of vehicles is mostly about controlling the air flow around a vehicle. The air flow around the vehicle can affect the vehicle's stability and drag. Furthermore, the appropriate vehicle design can tune the outer flow to prevent droplets of rain water from accumulating on the windows and mirrors, and keep headlights free of dirt and wind noise. Tuning the outer flow has not much effect on the fuel efficiency, therefore this text will be focusing only on reducing the aerodynamic drag.

The first section 1.3 shall go more detailed into fuel efficiency and the theory about aerodynamic drag. Section 2.2 shall go through the aerodynamic development of a vehicle. Section 2.3 shall go through the tools of aerodynamic analysis, like CFD in subsection 2.3.1 and wind tunnel testing in subsection 2.3.2.

2.1 The energy and fuel consumption

In both vehicles from DNV GL Fuel Fighter, the motor is electrical. In the Prototype the source of the motor is lithium battery, and in Urban Concept the source is fuel cells from hydrogen. From the motors' electrical power, it gets converted into mechanical power to overcome the resistance to motion. The process is shown in equation 1.1. A motor controller was made to make the running motor more efficient. The most fuel efficient driving cycle in the aspect of the motor is to drive up to maximum speed, and then shut down the motor for the vehicle to only roll. This driving cycle were also done in SEM, accelerating to max speed in 35 km/h and decelerating to 20 km/h and sometimes down to 0 km/h, because it has to stop in every laps. The expected average speed of 30 km/h throughout the track in figure 1.3 would be sufficient to make it within the time limit of 39 minutes.

The forces action on the vehicle is shown in figure 2.1, and the forces are, the aerodynamic drag D , tire resistance R , the vehicle weight W . According to newton's

law of motion the tractive force F_T between the tires of the driven wheels and the road are derivatived in equation 2.1.

$$F_T = D + R + m \frac{DV}{dt} + G \sin(\alpha) \quad (2.1)$$

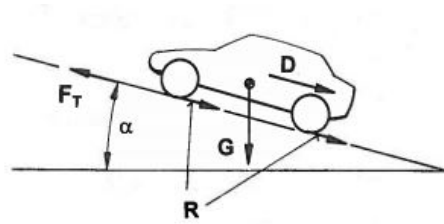


Figure 2.1: An illusion of the forces action on the vehicle [7]

The resistance forces from equation 1.1 are the tractive forces F_T . Equation 2.1 and figure 2.1 show that the vehicle is driving in a incline angle α , for simplification assumed no incline $\alpha = 0$. Then the only properties that can be changed in equation 2.1 are the aerodynamic drag D and the tire resistance R . There are several factors that affect the tires rolling resistance, such as rubber material, temperature, speed, etc. All these factors can be collected into the rolling resistance coefficient k_r . From Snyder [17] it was generally found that the rolling resistance R is nearly directly proportional to the downforce G (also known as the weight of the car) applied on the tire, see equations 2.2.

$$R = k_r * G \quad (2.2)$$

From equations 2.2 the only property that can be modified is the weight, because the rolling resistance coefficient k_r is fixed. The tires are special made by Michelin for SEM, and k_r is $1.5 \text{ kg/ton} = 0.00015$ which is really low compared to tires for passenger vehicles. The data of the Michelin tires for SEM can be found in appendix D. For low velocities like in this project, k_r doesn't change significantly [18, 17], therefore it can be assumed constant rolling resistance.

The flow around road vehicle is fully turbulent, and the flow can be described by the unsteady Navier Stokes' equation (NS). The NS expresses the equilibrium of inertia, pressure and viscous forces. The basis of solving aerodynamic incompressible flow are NS together with conservation of continuity and energy equations. NS are coupled, nonlinear, second-order, partial differential equations, which makes

it nearly impossible to solve NS algebraically. A more known and much more simplified equation for aerodynamic drag are shown in equation 2.3, which are found by experiment and dimensions analysis. Where D is the aerodynamic drag, ρ is the air density, A are the cross sectional area of the vehicle shown in figure 2.2, the dimensionless number, C_D drag coefficient, and the vehicle velocity V at still air.

$$D = \frac{1}{2} \rho V^2 A C_D \tag{2.3}$$

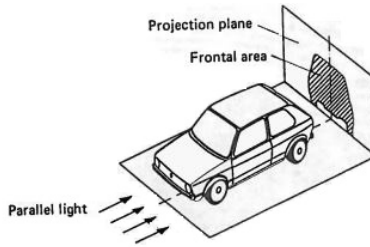


Figure 2.2: An illusion of the cross sectional area A [7]

Still ambient air is a rare condition in the real life, generally a wind is blowing with a speed v_w in random directions degree δ . The vector sum of the vehicle speed V and the wind speed gives the resulting "wind speed" V_∞ with the approaching yawing angle with the vehicle. This makes other forces in different directions and moments like yawing, pitching and rolling moments, which are much interested properties in aeronautics industry. But for automotive industry only the overall the tangential force T a force of interest, therefore will throughout this text a still ambient air be considerate. Figure 2.3 shows the wind velocities vectors. Throughout this text it will be simplification of still ambient air.

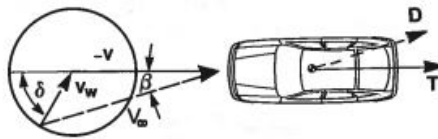


Figure 2.3: An illusion of the wind velocities vectors [7]

Equation 2.3 shows that the aerodynamics drag depend on the velocity in the power of 2, and therefore, that it also depends strongly on the driving cycle. To have the least amount of aerodynamic resistance the vehicle should drive in a very low

speed. But the driving cycle are already set by the motor efficiency and the SEM rule, where the average velocity is 30 km/h.

As shown in figure 1.6 the aerodynamic drag comes from pressure drag and skin friction. For a typical vehicle shape, pressure drag is the predominant compared to skin friction. The skin friction is the friction between the interaction of the molecules from the air and the vehicle surface. A smoother surface give less skin friction than a rough surface.

The pressure drag are also called form drag, because the form (shape) of the vehicle makes the air flow impose a pressure distribution around the vehicle. A steep pressure difference will give separation, and reattach air flow, which impose higher aerodynamic drag. There are two different types of separations. In type 1, the separation line is perpendicular to the flow, and vortices are generated. This usually happens because of hard edges on the vehicle. In type 2, the flow separation is characterized by separation line inclined with respect to the oncoming flow, because of the rear end shape of the vehicle. Figure 2.4 shows an illustration of the two flow separation types, where separation type 2 figure 2.4a are shown in aerial perspective.

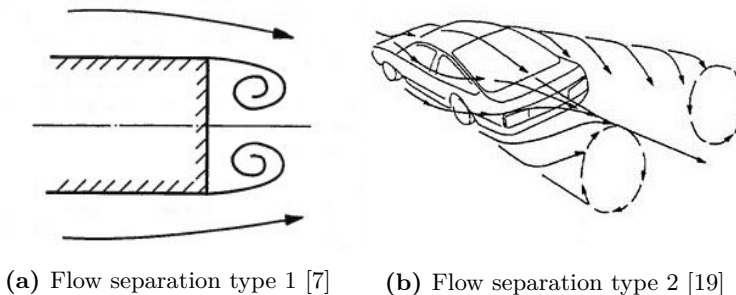


Figure 2.4: An illustration of the two flow separation types

2.2 Aerodynamic Vehicle Design

Generally there are two ways of designing low drag vehicles; a radical approach and a more conservative approach. The radical approach takes a known low-drag shape, like the tear drop shape from Scibor-Rylski (figure 2.5), and modify it to a driveable vehicle. This is the typical design approach for the Prototype class in SEM, as figure 1.1 illustrated 1.1. The second approach is more conservative; it starts with a vehicle design, and reduces its drag by gradual modifications.

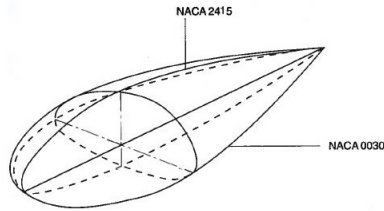


Figure 2.5: Scibor-Rylski ideal shape based on NACA2415 and NACA0030 [8]

The aerodynamic drag is proportional to the vehicle's cross sectional area A and the drag coefficient C_D , from equation 2.3. Hence, to minimize drag the cross sectional area and the drag coefficient have to be minimized.

The cross sectional area is determined by the dimension restrictions in the SEM rules and regulations article 45 [11]:

- The vehicle highest point must be between 100 cm and 130 cm.
- The vehicle widest width, excluding rear view mirrors, must be 120 cm and 130 cm.
- The total vehicle length must be between 220 cm and 350 cm.
- The width between the tires must be at least 100 cm for the front axle and 80 cm for the rear axle, measured between the midpoints of the tires when touching the ground.
- The wheelbase must be at least 120 cm.
- The Driver's compartment must have a minimum height of 88 cm and a minimum width of 70 cm at the Driver's shoulders.
- The ground clearance must be at least 10 cm with the driver (and necessary ballast) in the vehicle.
- The maximum vehicle weight (excluding the Driver) is 225 kg.

The drag coefficient C_D is a dimensionless number that measure the flow quality around the vehicle. Since the drag coefficient is a dimensionless number, it can compare the aerodynamics properties of different shapes, inclination and flow conditions

[20]. The flow around a vehicle has typically steep pressure gradient, separated and reattached flow and some lateral streamline to direction of flow [7]. A minimized drag coefficient has no steep pressure gradient, separated flow and no rear end wake, where the streamlines are perfect streamlining, like the flow over the airfoil in figure 2.5. While the streamline over the sphere has the flow separation type 2.

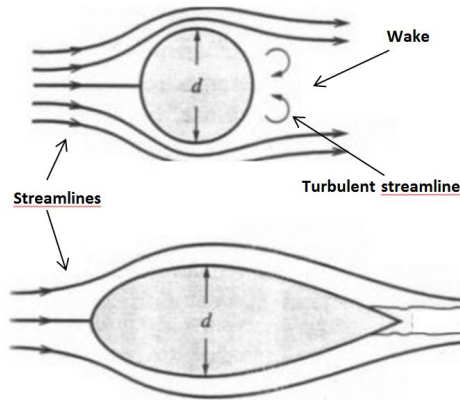


Figure 2.6: Streamline around a sphere and an airfoil, and their respective drag coefficients [9]

2.3 Tools of aerodynamic analysis

The shape of a vehicle is "frozen" very early in the course of development, so good aerodynamics properties have to be worked into the very first design stages of a new vehicle, making use of both past experience (intuition) and, further experimental analysis. For further analysis there are three possible methods; Real road testing, wind tunnel testing and computational analysis (CFD). Each of these have advantages and limitations.

Real road tests offer the advantage of realistic conditions, but it is really expensive and time consuming, because one has to build a running model of the design. Further drawbacks are the difficulty of reproducing test conditions, difficulty of securing confidentiality, and the difficulty of making measurements.

The advantages of the wind tunnel are that the experimental time is really fast, and that the test conditions are easier to monitor and control. The drawbacks are that building a wind tunnel and running a wind tunnel are both very expensive. Also, making a model of the car for the purpose aerodynamics analysis only, is not cost efficient.

Computational Fluid Dynamics (CFD) is a digital aerodynamic analysis method. It is widely used in the automotive industry, because of the highly demand of cost efficiency. CFD gives a useful graphical display of issues like pressure and velocity distribution, streamlines, and etc. Therefore, CFD is a good tool for aerodynamic comparison of different design concepts. Although CFD is time consuming, all that is needed of material (for our purposes) is a personal computer with CFD software.

In the project, both CFD analysis and wind tunnel testing where carried out. This was because of the characteristic differences between them, making them complementary rather than directly competitive. CFD always gives an answer, but getting the right answer is not always as easy. Verification and validation is really important in CFD, to test the accuracy of the CFD answer. **Validation** is defined as the process of determining the degree to which a model is an accurate representation of the real world from the perspective of the intended uses of the model. **Verification** is defined as the process of determining that a model implementation accurately represents the developer's conceptual description of the model and the solution to the model. [21, 22]. The validation of CFD results were done with wind tunnel testing.

The road vehicle displaces the surrounding air with its movement, which means the air is stationary and the car is moving. But during simulations in CFD and wind tunnel testing the car is stationary and the air is flowing. This is due to the fact that a force equilibrium exist at every point on the body surface and the air interface (Newton's third law of motion). It is immaterial to the simulation whether the vehicle moves and air is stationary or just the opposite.

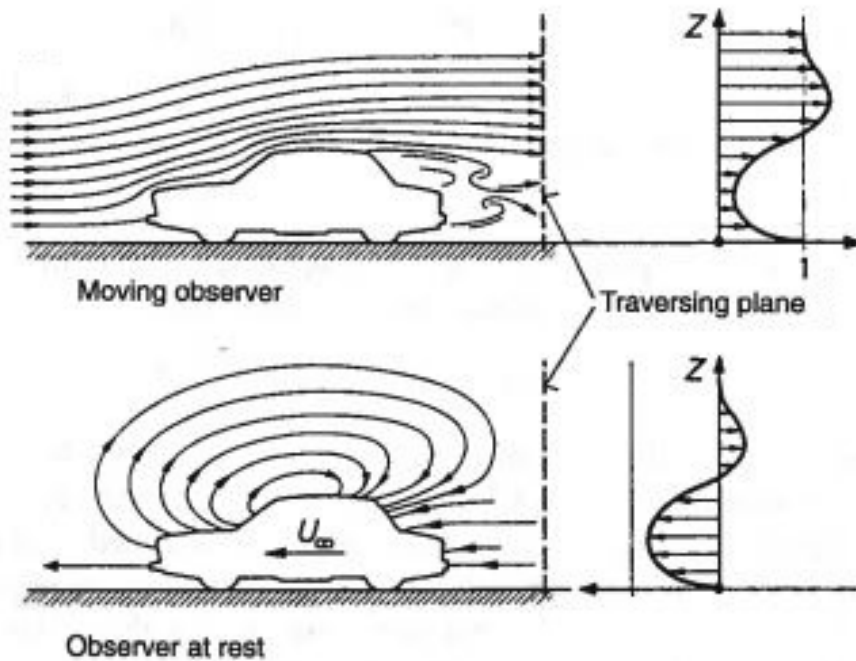


Figure 2.7: The difference in relative motion between road driving and CFD and wind tunnel testing [7]

2.3.1 CFD

Computational Fluid Dynamic (CFD) is a computer software that solves NS numerically. To solve a problem numerically, the problem has to be discretized, which means breaking the problem into smaller parts, solve it and superimpose the answers.

The CFD software are divided into two parts; post processor, solvent processor and. Before doing CFD modelling a digital model of the vehicle has to be made, typically in CAD (Computer-aided design) - software. There are three basic steps in CFD modeling;

1. Discretization of body surface or the computational domain, called meshing or making grid, in the preprocessing software.
2. Choosing the calculation method, and solving the problem, in the solvent processor.
3. Making suitable graphical display in the post processing software.

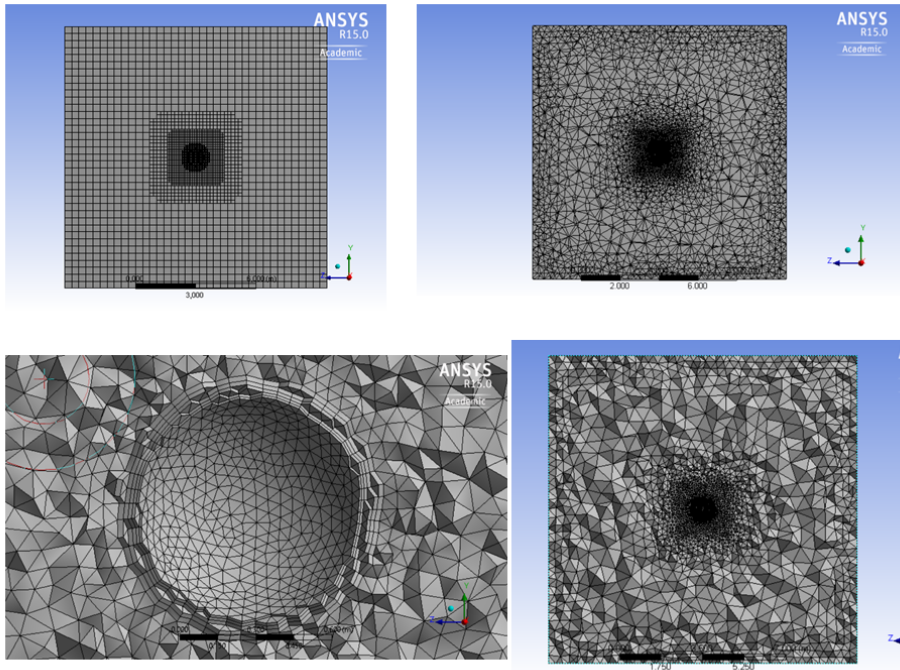


Figure 2.8: The different mesh done on a sphere

The CAD model for CFD has to be simplified, as a complex geometry with hard edges and sharp angles could give high skewness of the mesh, which could make it take longer for the result to reach convergence, or maybe even give the wrong results. Orthogonality and the aspect ratio of the mesh could also affect the amount of iteration for convergence. The skewness should be low, the orthogonality should be high, and the aspect ratio should be as close to 1.

The finer the mesh is in the post processor, the more accurate is the answer, but the more computer memory it needs. To save the computer memory, it is possible to make the mesh finer in the area where flow is changing much, like in the wake area, at surfaces of the body, etc. Making the right mesh takes time and experience. The author tested the CFD skills on a known geometry, like a sphere, before CFD-analysing the vehicle. Figure 2.8 are showing the different choices of mesh for the CFD calculation of a sphere.

There are different CFD methods to compute NS, and more accurate answers generally demand more CFU. This list of CFD methods is sorted in increasing order of effort:

1. Linear Methods

- a) Vortex Lattice
- b) Panel Methods

2. Non Linear Methods

- a) Inviscid Euler Method
- b) Reynold Average Navier Stokes Method (RANS)
- c) Unsteady viscous
 - i. Large Eddy Simulations Method (LES)
 - ii. Direct Numerical Simulation Method (DNS)

The different method can be read about in for example the textbook of Hucho [7]. The most classical CFD approach to describe turbulent flow (which are typical around a vehicle) is RANS.

A turbulent flow makes the velocity and pressure a function that depend not only on space (x,y,z), but also on time (t). In RANS method, the flow is split into a time-invariant mean motion and time-dependant motion. Equations listed in 2.4 gives expressions for velocity components and for pressure. u is the velocity in x-direction, v is the velocity in y-direction, w is the velocity in z-direction, and p is the pressure. The bar over the values indicates mean, and the prime indicate the fluctuating time-dependend part.

$$u = \bar{u} + u'; \quad v = \bar{v} + v'; \quad w = \bar{w} + w'; \quad p = \bar{p} + p' \quad (2.4)$$

This introduces to new variables which are called Reynolds stresses, where the Reynolds stresses can be calculated by turbulence modelling. There are a lot of different turbulence models, the most known and capable model for turbulent vehicle flow are the k- ϵ turbulence modelling.

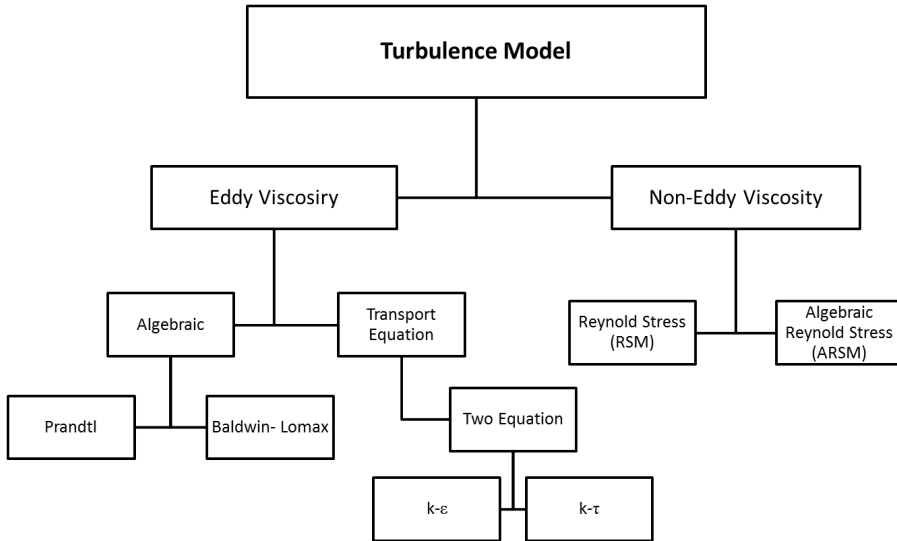


Figure 2.9: A brief hierarchy of the turbulence model

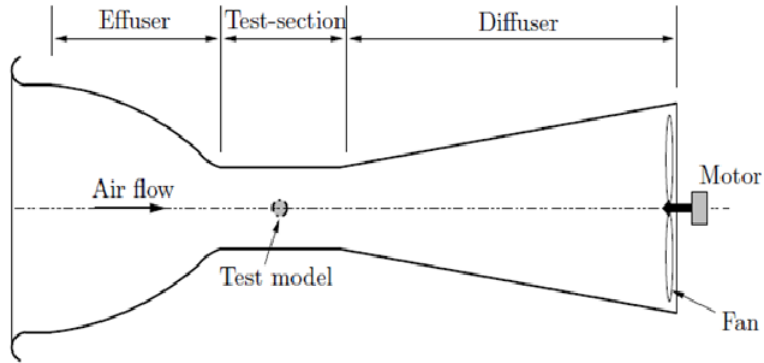
A numerical solution always gives a mathematical error, but the choices of the mesh and the solvent solutions make could minimized the error. The error depends on the user demand of the accuracy of the result, the CPU-time and the computer memory. Because CFD results depend much on the user's experience, verification and validation are important steps in CFD.

2.3.2 The wind tunnel

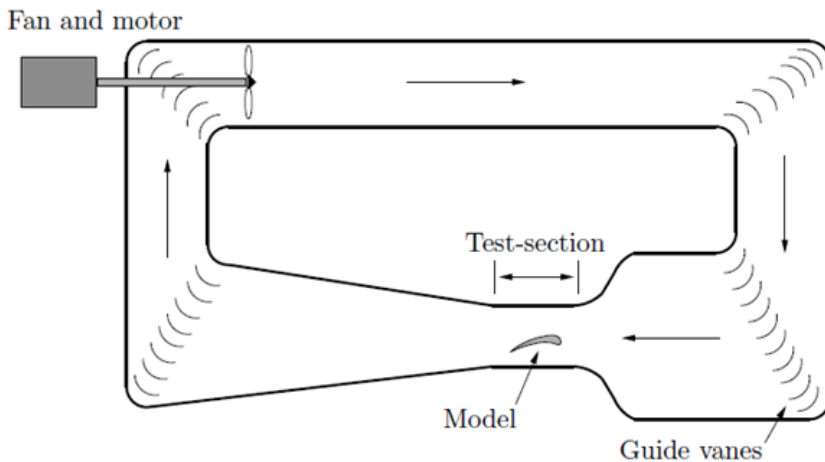
A wind tunnel simulates the conditions on the road, by physically producing a flow. Like for most simulations, there are always some differences from the reality. For example the temperature field above the road is not always homogeneous. Intense sunlight will heat the surface of the road more than the surrounding air, generating a temperature boundary layer above the road.

There are three types of wind tunnel configurations; the closed circuit tunnel and the open circle tunnel. In the closed circuit tunnel, as the name indicates, the wind turbine drives the air within a closed circuit. In the open circle tunnel the turbine drive the flow back into the surroundings. Figure 2.10 shows the open circuit

tunnel and closed circuit tunnel. Both wind tunnel types has their advantages and disadvantages that can be read more about in pp.633 in the book of Hucho [7].



(a) An open circuit wind tunnel



(b) A closed circuit wind tunnel

Figure 2.10: An illustration of the two wind tunnel types [7]

Both Figure 2.10 shows that the wind tunnels have a **test section**, which is an important factor when considering similarities with the road. The test section's wall can affect the flow of the tested object. The ratio between the test section's cross sectional area and the the tested object is called **blockage ratio** φ , and should be a small as possible. The acceptable blockage ratio for automotive wind tunnel testing is $\varphi = 0.10$.

There are some correction equations for high blockage ratio, but there is also the

possibility of making a smaller model (scale model). Another advantage of making a reduced scale model is that it's also cheaper. From the Buckingham Pi dimension analysis done in appendix C, the drag coefficient are only dependent on the Reynolds number. Which means for similarity the Reynolds number should be the same in the real situation and the scaled situation, to get the same forces. Equation 2.5 shows the derivation of the Reynolds number. Re is the Reynolds number, ρ the air density, L_c the characteristic length (which is the reference length) and μ the air viscosity.

$$Re = \frac{\rho L_c V}{\mu} \quad (2.5)$$

To find the drag coefficient, four factor is needed to be known from equation 2.3; the aerodynamic drag, the velocity of the flow, the flow density and the cross section of the car. Where all the factors are found, they can be analysed to find the drag coefficient by a calculation software e.g Microsoft Excel, Matlab and etc.

The measurement of the aerodynamic drag (including other forces and moments) are done by a balance plate. The Beam scale is the most popular wind tunnel balance plate. When the Beam tilts downward, a motor in the Beam automatically shifts the running weight in the counter direction until the Beam is balanced again. Where the electrical voltage from the Beam motor get measured for further analyse. The Beam scale needs to be calibrated to find a relationship between the electrical signal and the different known forces acting on the Beam scale. Where the relations should be linear, acceptable determination factor R^2 are between 0.95-1.

In the wind tunnel the velocity of the flow is not measured, but the pressure pressure is measured by a Pitot tube. The Pitot tube has an membrane that measures the static and dynamic pressure, where a transducer converts the pressure on the membrane to electrical signal in voltage. Also the Pitot tube need to be calibrated, where the relationship between the different flow pressure and traduce voltage are found. The velocity is found by derivation the Bernoulli's equation 2.6. Where P_0 is the static pressure, P is the dynamic pressure, V_0 is the velocity at static pressure, which is zero and therefore gives the velocity equation 2.7.

$$P_0 + \frac{1}{2}\rho V_0^2 = P + \frac{1}{2}\rho V^2 \quad (2.6)$$

$$V = \sqrt{\frac{2(P_0 - P)}{\rho}} \quad (2.7)$$

There are different ways to measure the density of the air flow and cross sectional area of the vehicle. The air density can for example be found the mercury pressure meter, by using the air density and mercury ratio. The oldest technique to measure the cross sectional area is probably shadow-measuring, as illustrated in figure 2.2. In this case, the contour of the shadow is drawn and then calculated analogously. This analogue calculation could give some human errors. In modern times a CCD-camera is mounted and a Marata screen is inserted between the vehicle and the camera. The shadow forming on the Marata screen is digitized and a computer software can calculate the cross sectional area.

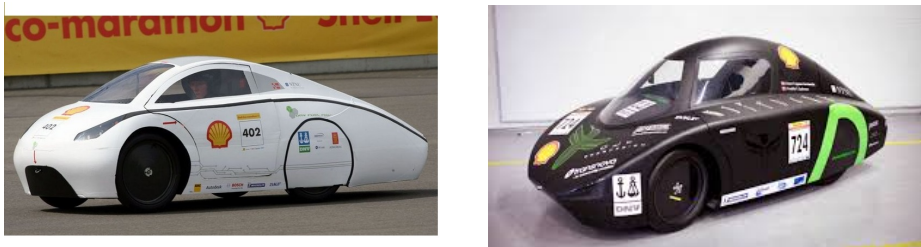
Chapter 3

The vehicle design approach

This chapter will go through the aerodynamic aspect of phase 3 in the IPM methodology. Section 3.1 shows the two concepts chosen for further aerodynamic analysis. Section 3.2, 3.3 and 3.4 shall go through the aerodynamic tool's set up that been used in this project. Where section 3.2 concerns the intuitive aerodynamic analysis, section 3.3 is about CFD analysis, and the results are validated in section 3.4 by wind tunnel testing.

3.1 The design concepts

Figure 3.1 shows the two former Urban concepts made by NTNU students. Figure 3.1a shows the car from 2009 and figure 3.1b shows the car from 2012. These two vehicle have the smallest cross sectional permitted by SEM's rule and they are quite well streamlined with slender rear ends.



(a) Urban Concept from NTNU 2009 [23] (b) Urban Concept from NTNU 2012 [24]

Figure 3.1: The two previous NTNU Urban Concepts

This year's team decided to build a car that was totally different from previous cars. Where the mission was "to make a new Urban Concept that has the potential to win the Design Award", which could come at the expense of the aerodynamics aspect. But at the same time the vehicle is going to compete in SEM, which is

about fuel efficiency. And, as the aerodynamics drag is a big contribution to fuel consumption, aerodynamics was apart also a part of the IPM methodology process.

In phase 3 in the IPM methodology the team started with sketches, and two concepts were chosen for further analysis. These sketches of Concept 1 and 2 are shown in figure 3.2 and 3.3, respectively. Both concepts have a sports look, that appeal much to the general public. And the mirrors are inside to minimize the cross sectional area and flow separations. The Concept 1 looks like a race car, with the front wheel hanging outside of the body. The concept 2 gives the illusion of bigger wheel and lower center of gravity.

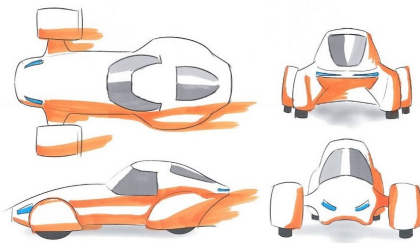


Figure 3.2: Concept 1

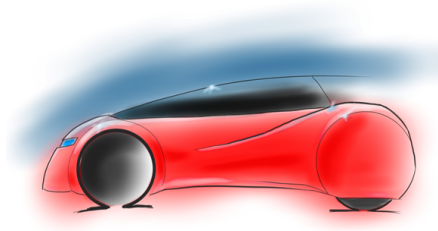


Figure 3.3: Concept 2

3.2 The intuitive aerodynamic analysis

The intuitive aerodynamic analysis of Concept 1 was that the front wheels would give a steep pressure difference. The stalk connecting the body and the wheel, would give additional flow separation. To minimize flow separation from the stalk, a streamline modification was done, shown in figure 3.4. This modification changed the design much, so much that the team did not agreed on the modification. Hence, the modification didn't get further analysed.

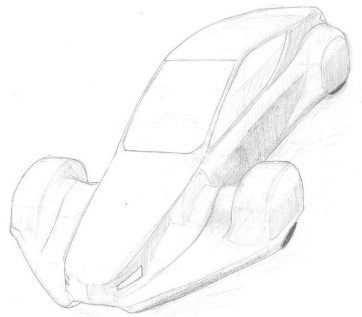
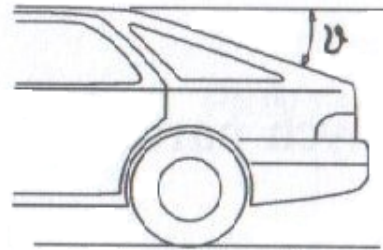


Figure 3.4: Aerodynamic modification of concept 1

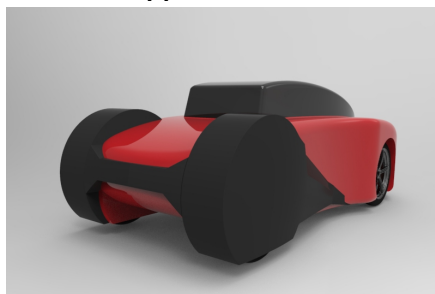
The aerodynamic intuition for Concept 2 was that the rear end had a typical notchback configuration. Figure 3.5 gives a comparison between notchback and hatchback rear ends. Figure 3.6 shows a graphical display of the relationship between drag coefficient ratio and the effective rear angle slope for notchback and hatchback, with data from different researchers. The effective rear angle slope is; from the horizon to the slope of where the rear end starts to be too steep to the end of the car, like in figure 3.5b. And the drag coefficient ratio is a normalisation, between the drag coefficient at that rear angle and the drag coefficient when the rear angle is zero. From the figure 3.6 it is clear that a hatchback has less drag coefficient, because a notchback configuration gives bigger wake and flow separation than a hatchback. Changing the rear of Concept 2 to another configuration would give a change of the design too big for the team to accept. But the effective notchback rear end angle of the Concept 2 is 23° , which gives quite low drag coefficient compared to other angles, shown in figure 3.6.



(a) An illustration of notchback [8]



(b) An illustration of hatchback [8]



(c) A digital figure of the Concept 2 [25]

Figure 3.5: The figures show the notchback and hatchback configuration, for comparison

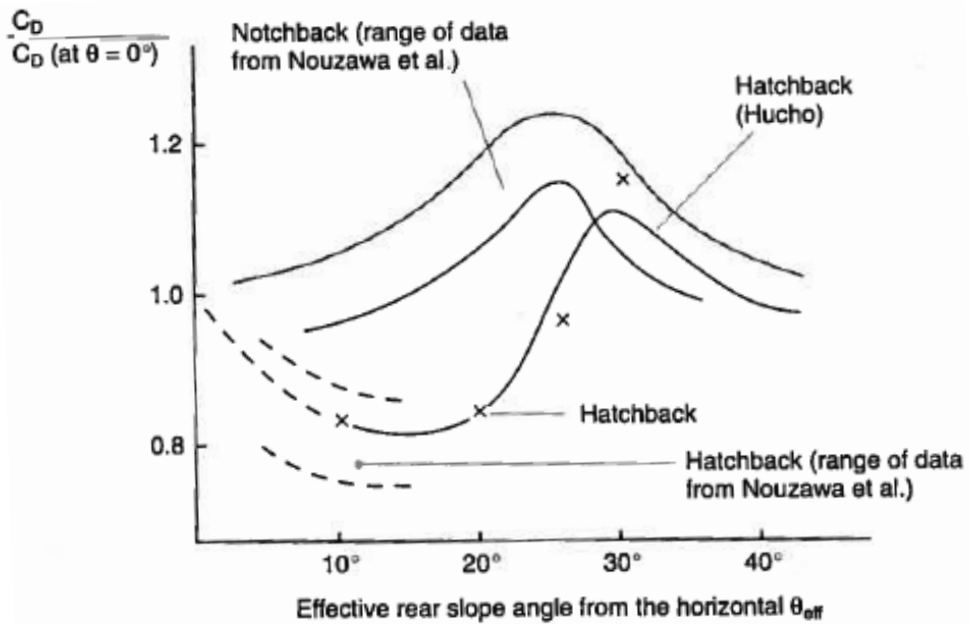


Figure 3.6: A graphical display of the relationship between the normalised drag coefficient and the effective rear end slope [8]

To make the Concept 2 as streamlined as possible, we took notice of the Rumpler Limousine from 1921. The Rumpler Limousine also had a notchback configuration, and a dome top compartment, shown in figure 3.7. The Rumpler Limousine had very good aerodynamic features because of the airfoil shape, so an airfoil dome configuration was also included in concept 2. The sides of the dome were of an airfoil shape, similar to NACA0030, which has the shape of the least drag coefficient, shown in figure 2.5.



Figure 3.7: The Rumpler Limousine of 1921 [10]

3.3 The CFD set up

The next step of aerodynamic analysis was carried out using Computational Fluid Dynamics (CFD). ANSYS Fluent 15.0 was the CFD software used in this project. This software has preprocessor, solver and post processor integrated. Fluent solver uses finite volume as the discretization method, which is good for high Reynolds numbers, usage of memory and solution speed. The finite volume method derive the partial differential equations; NS, the mass and energy conservation equations, and turbulence equations, into potential functions. [26, 27]

The CAD model of the different concepts, were modeled in Siemens NX 9.0. The CAD models were simplified with no hard edges and just one connecting body including the wheels. This is shown in figure 3.8. A rotating wheel affects much of the flow field and could also affect the drag coefficient. Simulation of the flow field around a rotating wheel is quite difficult, because it needs partly moving mesh. In the automotive industry, the effect from the rotating wheels is simulated by installing a running treadmill in the wind tunnel. Another less expensive method is to have different height from the ground in different simulation speed. This is because the flow interference with the ground makes a turbulent boundary layer, having similar to effect as the rotating wheels. This text is going to use the expected average speed of 8.33 m/s (30km/h), which requires a 10 cm clearance from the ground. [28, 29]

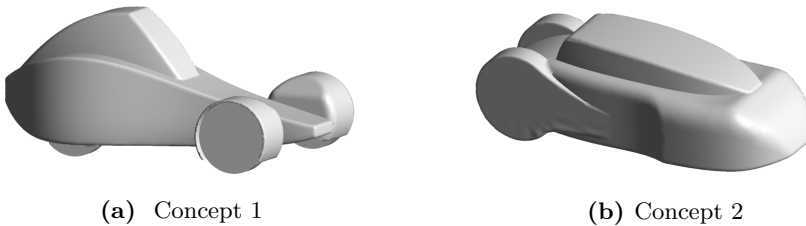


Figure 3.8: A simplified CAD-model of both concepts

Because the validation of the CFD result are in a wind tunnel, CFD set up shall be similar set up in the wind tunnel. To have a good computational domain for the flow around a vehicle, the inlet should have at least three car-lengths in front the vehicle, and five car-lengths behind the vehicle. Both vehicle design concepts were 3.00 m long, which correspond to an inlet at 9.00 m in front of the car, and an outlet 18.0 m behind the car. This is for avoiding interfering of the flow around the car. The domain behind the car is bigger than the domain in front of the car; this is because of the wake. The side wall was 1.00 m from the center of the car in the vertical direction, the domain height was 1.10 m.

Since the car is symmetric along the center of the longitudinal direction, the flow would also be symmetric along the longitudinal direction. To save CPU time and computer memory, the calculation domain was cut along the center of the car in the longitudinal direction, as shown in figure 3.9. The post processor can then mirror the domain to calculate and show the complete results.

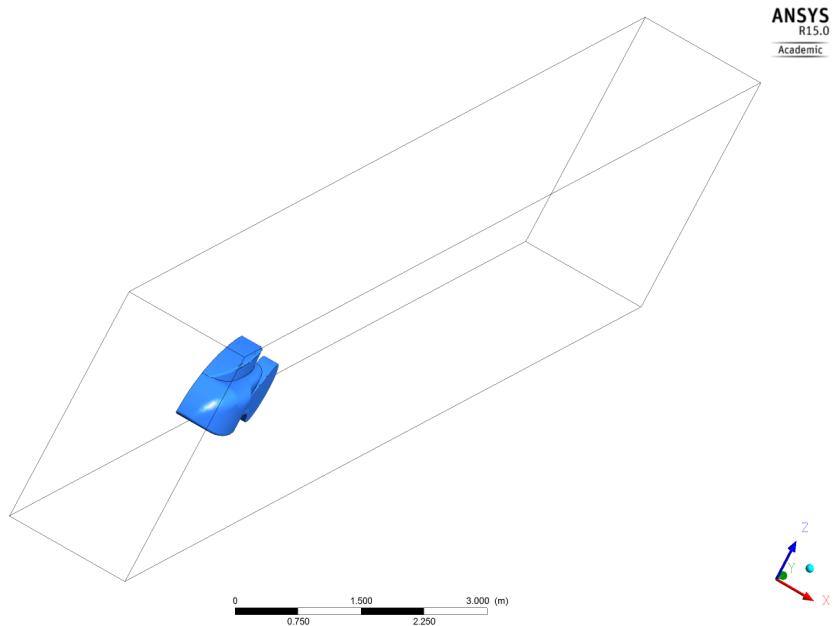


Figure 3.9: The computational domain, where it got cut in the longitudinal direction the vehicle

In the preprocessor of Fluent the discretization mesh was made. The overall mesh in the domain had a non-structural triangular mesh. The surface of the ground and the car had prism layer inflation with first aspect ratio of 5, growth rate of 1.20 and 5 inflation layers. A square cuboid around the car with and 1 car-length behind the car was made. The cuboid had 10 % finer mesh than the rest of the domain, as shown in figure 3.10. Also the area behind the wheels' capsule, notchback, stalk and etc, had a 20-100 % more refined mesh. These areas were refined because the flow is expected to change here more than the rest of the domain. Figure 3.10 shows the refined mesh area and the inflation mesh on the surface of the vehicle and the ground.

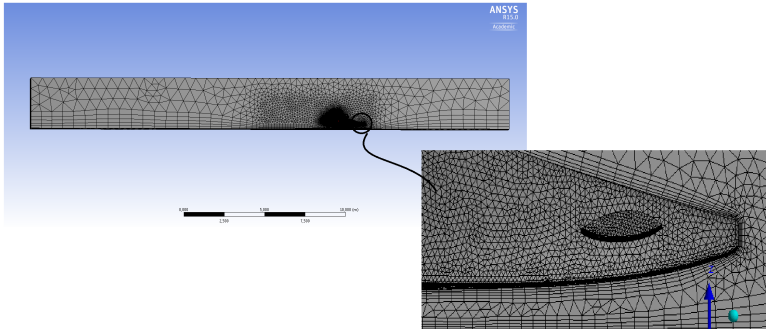


Figure 3.10: The refined mesh area, with zoomed mesh to show the inflation mesh on the surface of the vehicle and the ground

Table 3.1: Boundary conditions and assumptions for the simulations of the two concepts

Boundary	conditions	assumptions
Inlet	Velocity inlet 8.33 m/s with 1 % turbulent intensity	Constant uniform velocity, no wind nor side winds
Outlet	Pressure outlet at ambient air with 5 % turbulent intensity	No back flow
Road	No slip wall condition	No moving road
Longitudinal plain	Symmetry plane	Symmetrical flow along the longitudinal plane of the car
Top and side domain	Specific shear wall or no slip condition	Big enough domain to not affect the flow

An assumption was made of no side winds and still ambient air. These are not realistic assumptions, but for comparison between two designs, and to see the aerodynamics characteristics, it is a justified simplification. Also the boundary conditions were the same on both concepts. The inlet was set to be uniform flow with the velocity 8.33 km/h and 1 % turbulent intensity. The outlet was set to

pressure outlet at ambient air, with 5 % turbulent intensity. If the outlet has back flow it means the outlet were set too close to the vehicle. The road was set to no slip wall condition with no moving boundary, like in the wind tunnel. The plane at the longitudinal direction of the car, was to be the symmetry plane, which is the as specific shear wall condition. The top and the side domains were set to be specific shear. Table 3.1 show a summary of the boundary conditions with the assumptions.

The chosen solvent was RANS method with the turbulence model realizable $k-\epsilon$ which would achieve good result in term of integral value, e.g. drag coefficient [30, 31], which were the properties of interest. The wall function was set as non-equilibrium, since it is good at accounting separated and reattached flow, without a significant increase in either CPU-time or dynamic memory [31]. A pressure-based solver with couple scheme and least squared cell based solutions method were set, because the solution converges faster for low-speed incompressible flow. In the pressure-based solver the pressure field is extracted to continuity and momentum equations. For even faster convergence, the 100 first iterations had first order upwind momentum, turbulent kinetic energy and turbulent dissipation rate [32]. The next 1000 iterations were in second order for all of the three equations.

3.3.1 Discussion and comparison of the CFD results

The verified results are shown in table 3.2. There where five different steps of verifications:

1. Checking the mesh structure
2. Velocity residues in the order of at least 10^{-03}
3. Convergence, with at least three number of significant digits for the drag coefficient
4. Net mass flux between inlet and outlet
5. Grid independence test

Checking the mesh structure was to see if the mesh was compatible with the simulations. If the minimum volume of the mesh are negative, which is not physically possible, it would give an incorrect answer. The orthogonality and the skewness of the mesh were also checked for faster convergence. In ANSYS Fluent the mesh quality could already be checked in the preprocessor, while making the mesh. The average orthogonality and the skewness of the mesh for both car designs were around 0.85 and $3.0e-04$, receptively.

Residues of the velocities at least in the order of 10^{-03} . If the residues are in smaller order, more iteration is needed, or one must change the CFD set up. This is important because the velocity is what the CFD is calculating.

Convergence, with at least three number of significant digits for the drag coefficient. Even though the residues of the velocities are at least in the order of 10^{-03} , the drag coefficient needs also to converge.

Net mass flux between inlet and outlet should be close to 0, to validate the continuity equation. The acceptable difference of net mass flux were in the order of 10^{-05} .

Grid independence test is to see if finer mesh would still have the same number of significant digits for the drag coefficient, because finer mesh gives more correct answer. For this project the changes after three number of significant digits was acceptable.

Table 3.2: The simulation results with the according amount of mesh elements

(a) Concept 1			(b) Concept 2		
no.	Elements	C_d	no.	Elements	C_d
1.1	789 475	0.3243	2.1	1 284 412	0.26333
1.2	852 594	0.3239	2.2	1 297 193	0.26574
1.3	1 329 335	0.325	2.3	1 652 211	0.26581

Both vehicles have good aerodynamic features compared to passenger cars, which

A normal passenger cars have drag coefficient between 0.30-0.45. In the resent five years there has been occasionally found passenger cars with drag coefficient down to 0.25, which are close to say that is not "normal" passenger car [33, 34]. The Concept 1 and 2 have the drag coefficient 0.32 and 0.27, from which it can be concluded that they have good aerodynamic features compared to passenger cars.

Table 3.2 shows that Concept 1 has higher drag coefficient than Concept 2. The reason could be because of the pressure distribution on the vehicles. Figure 3.11 shows the total pressure contours on the vehicles. The warmer colours (e.g red) show higher pressure and the colder colours show lower pressure. Figure 3.11 shows that the Concept 1 has more areas of steep pressure differences, such as in front of both wheels, the small front area and the on the body. Meanwhile, Concept 2 has only two steep pressure areas, in front of the car and at the rear end of the dome.

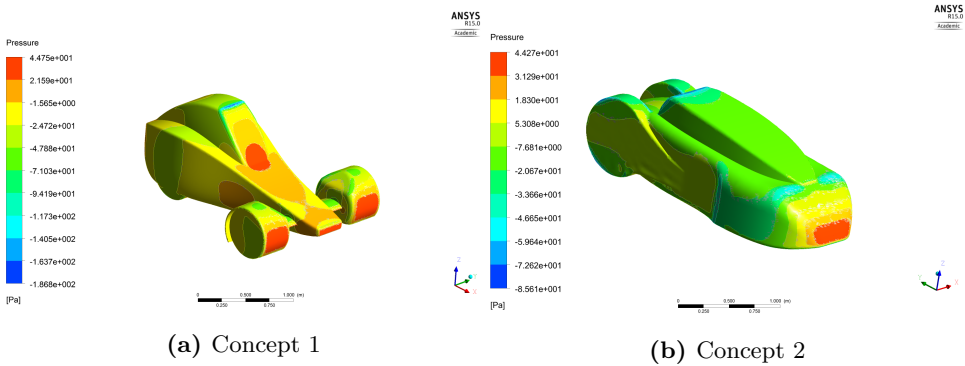


Figure 3.11: Total pressure contours on the vehicles at 30km/h

Figure 2.6 shows the streamlines of Concept 1, at the symmetry plane. The Concept 1 could reduce the drag coefficient by redesigning the rear end of the vehicle to reduce the wake, where the wake is shown in figure 3.12a. Figure 3.12b and figure 3.12c show the flow separation by the wheels, as suspected by seeing the pressure contours.

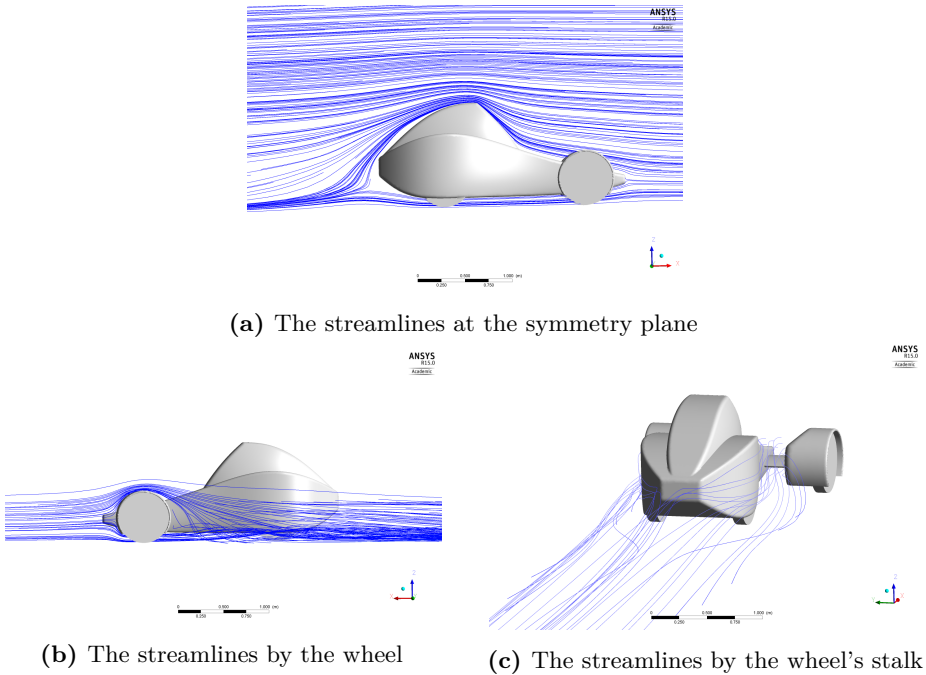
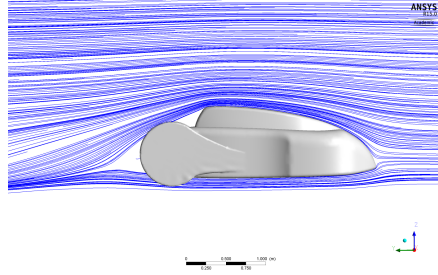
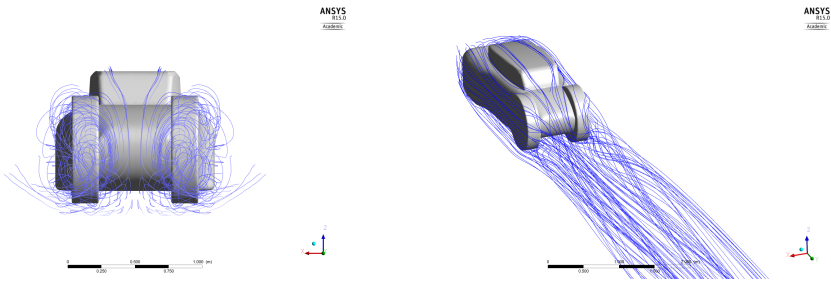


Figure 3.12: The streamlines of Concept 1

The streamlines of Concept 2 in figure 3.13 shows a bigger wake than concept 1, which is as suspected because Concept 2 has a notchback configuration. Figure 3.13b and figure 3.13c show the streamlines behind the Concept 2 in different views, which has the type 2 flow separations.



(a) The streamlines by one half of the car, in longitudinal direction



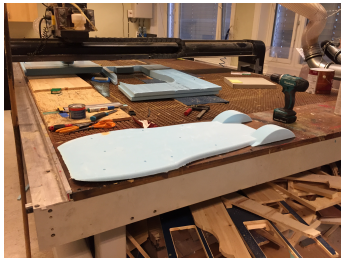
(b) The streamlines and the rear end of the vehicle (c) Different view of the streamlines and the rear end of the vehicle

Figure 3.13: The streamlines of Concept 2

With both concepts each one of them had their advantages and drawbacks; one of them had better pressure distribution and an other had better streamlines. The drag coefficient values 0.27 and 0.32 are so close that it can be said to have the same value, because the drag coefficient value 0.05 is insignificant. By aerodynamic analysis both concepts are capable. The choice of the concept ended on phase 4 in chapter 4.

3.4 Validation by Wind tunnel testing

To save money and time, only Concept 2 was validated through wind tunnel testing. Concept 2 was chosen because both concepts have the same CFD set up while Concept 2 has smaller drag coefficient. The wind tunnel testing was carried out at the department of Energy and Process Engineering (EPT) at NTNU, with a closed circuit wind tunnel type. There are two things that have to be done before the wind



(a) The milling process of the scaled model



(b) Scaled model of Concept 2

Figure 3.14: Pictures of the scaled model

tunnel testing; (1) making a physical model, (2) calibration of the Beam scale and the Pitot tube.

Since money and time are crucial factors, a 0.33 physical scaled model was made. The test model was milled out of the material styrofoam, in the milling machine at the "Prototype lab" in the IPM department, as shown in figure 3.14a. The CAD model of the Concept 2, in steep-file, was divided into 10 cm thick pieces in the vertical direction, because the styrofoam plates were 10 cm thick. The machine milled the plate one by one. The carved styrofoam pieces were glued together with styrofoam-glue. A lot of time was needed to polish and spackle the pieces, to get a smooth surface. It was important to be gentle because the material styrofoam is quite porous. Afterwards the model got foiled with a 3M Scotchprint material, which is the same material used on the new Urban Concept. Figure 3.14 shows the foiled scale model in the wind tunnel.

The calibration of the Beam scale and the Pitot tube are done in the same way as explained in section 2.3.2. The forces added on the Beam scale were done by adding mass on the scale and calculating the acting weight forces. Appendix E and F show the calibration data of the Beam scale and the Pitot tube, respectively. The relationship by the Beam scale and Pitot calibration are found in equation 3.1 and 3.2. The determination coefficient R^2 are 0.99 and 1.00 for the Beam scale and Pitot tube, respectively.

$$y = 0.40x - 0.03 \quad (3.1)$$

Where x is the voltage differences and y the forces

$$y = 28.8x + 0.91 \quad (3.2)$$

Table 3.3: The wind tunnel results

RPM	Velocity [m/s]	Reynolds no	Drag [N]	Drag coefficient
100	2.24	1.56E+05	0.07	0.12
200	4.54	3.16E+05	0.57	0.24
300	6.94	4.84E+05	1.62	0.30
400	9.36	6.52E+05	2.83	0.29
500	11.7	8.15E+05	4.30	0.28
600	14.1	9.79E+05	6.10	0.27
700	16.5	1.14E+06	8.24	0.27
800	18.8	1.30E+06	10.6	0.27
900	21.2	1.45E+06	13.4	0.27

Where x is the voltage differences and y the pressure difference

In the experiment the Pitot tube was attached 63 cm from the wall, 46.6 cm from the ground and 105 cm from the inlet of the test area. The test area's cross section is 274 x 180 cm, which makes the Pitot tube far enough from the boundary layer. The model was placed on the Beam scale 640 cm from inlet, and the space behind the vehicle was 379 cm. The length of the scale model was 99.0 cm. Which are far enough away for the characteristic flow to not be interfered.

The average velocity of the vehicle during the competitions is 30.0 km/h, and the scaled model is scaled to a factor of 0.33, which means the flow speed had to be 90.0 km/h. The wind tunnel's flow flow speed are not known, only the wind tunnel's turbine speed. Therefore the experiment should be tested in different turbine speeds. The table 3.3 shows the different turbine speeds in revolutions per minute (RPM), with the calculated velocity, Reynolds number, drag and drag coefficient, while appendix I

As seen in the table 3.3 the flow speed didn't reach 90 km/h = 25 m/s, because the wind tunnel's turbine didn't manage to run at higher RPM. Figure 3.15 shows that the drag coefficient does not change much with higher velocity, which makes the assumption of constant velocity up until 25 km/h acceptable.

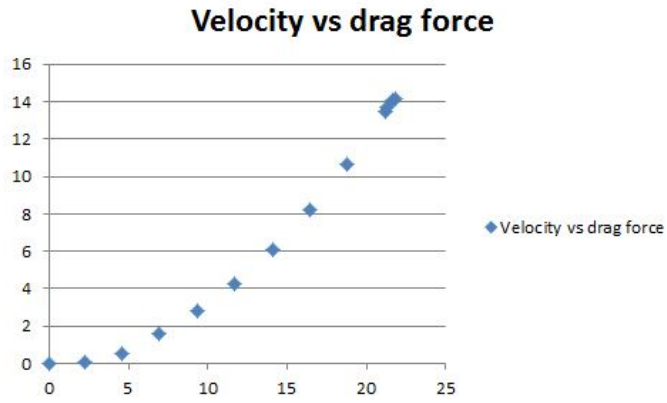


Figure 3.15: Reynolds number vs drag coefficient

Chapter 4

The new Urban Concept

This chapter will give a summary of the two last of the IPM methodology phases, more detailed description can be read in the overall report [12]. Section 4.1 and section 4.2, will go through phase 4 and 5, respectively. Section 4.3 concerns the end vehicle product and results.

4.1 Phase 4 - Structure and form

A normal passenger car usually divides chassis and body structures, but the new Urban Concept combined those two structure into what is called a **monocoque**. This structure saves a lot of material, which in turn significantly reduces the weight and cost. For strength calculation a more detailed CAD model was made in NX 9.0 for both concepts. During the strength calculation, it was found out that the Concept 1 was significantly more complicated than Concept 2 to manufacture. Choosing Concept 2 over Concept 1 was also supported by the finding that Concept two had a drag coefficient value 0.05 lower than Concept 1. Figure 4.1 shows the modelled CAD model of Concept with and without strength mesh.

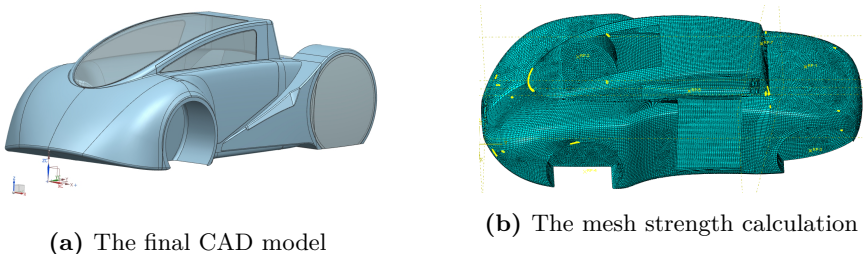


Figure 4.1: Detailed CAD figures from Siemens NX 9.0

Following the SEM rules, the vehicle is dimensioned for one person between 70-80

kg. This makes the vehicle quite small. Table 4.1 shows the dimensions of the car. The category "total vehicle mass" is including the motor, fuel cells and a full hydrogen bottle. The height, width and length are the outer dimensions of the vehicle.

The vehicle total mass	117 kg
The vehicle height	1.005 m
The vehicle width	1.300 m
The vehicle length	3.000 m

Table 4.1: Overview of the vehicle dimensions

4.2 Phase 5 - Production Preparation

In the production preparation, negative molds of the new Urban Concept were also modelled in NX. Figure 4.2 shows the modelled negative mold in six pieces. NTNU's milling machines were not big enough for carving the six negative molds. The company "Eker Design" in Fredrikstad Norway was kind enough to sponsor the team and lend equipment for the milling job of the molds.

The selection of material is crucial, and especially so for the monocoque. The choice ended up being carbon composite, reinforced with epoxy resin. This was already clarified in phase 2 by the morphology table shown in appendix J. The carbon composite fiber was applied on the negative molds. This was a demanding job, because the different carbon fiber waves had to be placed in the right place and in the right way, for the monocoque to be strengthened correctly. Figure 4.4 shows the six different carbon fiber waves, that were used in the monocoque. Afterwards, the mold with the carbon fiber was vacuum packed to add pressure, which forced the carbon fiber to fuse with the mold. And later the molds with the carbon fiber were placed in an oven, to heat the carbon fiber and make it stiff.

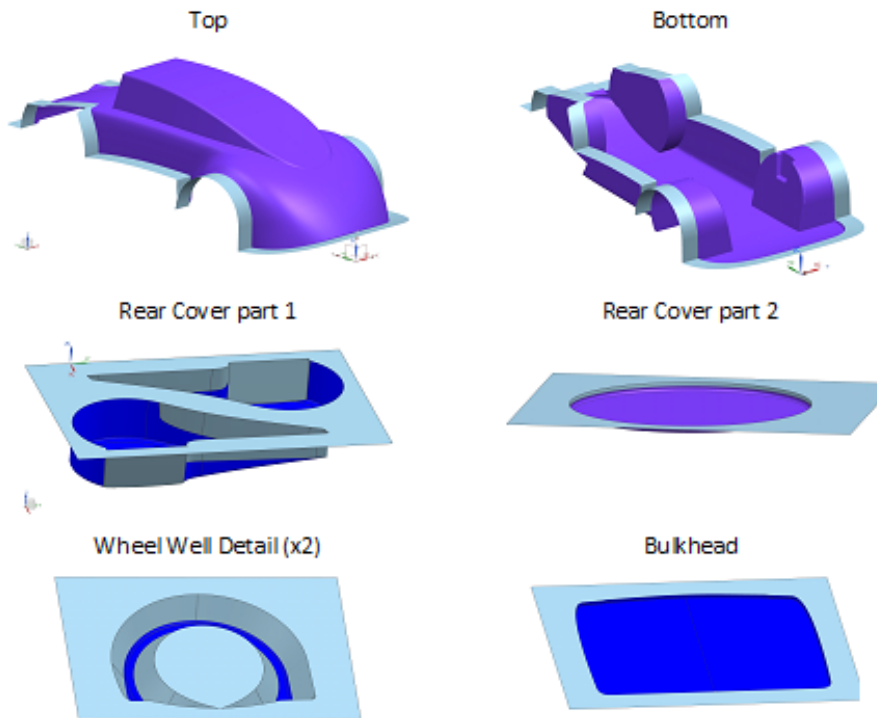


Figure 4.2: The negative molds of the vehicle in 6 pieces for production

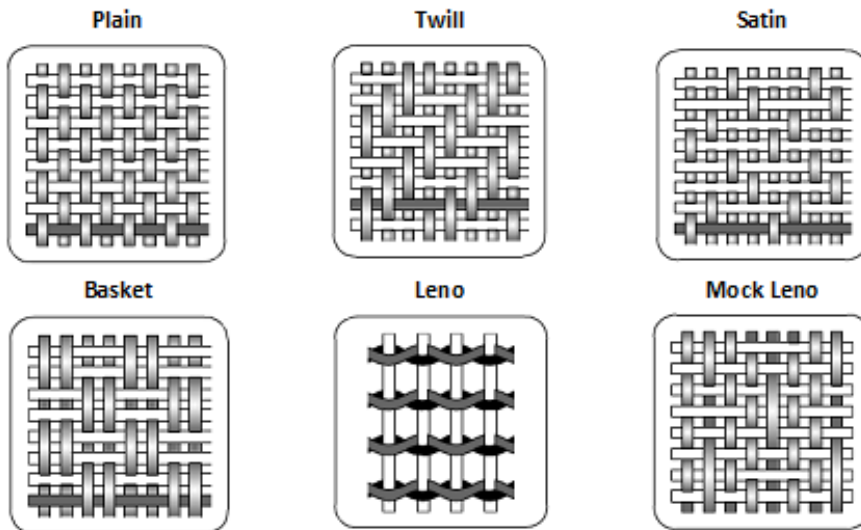


Figure 4.3: A figure of the carbon fiber weaves

The carbon pieces from the mold were glued together to make the final monocoque. Afterwards, almost two months were spent on polishing and sparking the monocoque to get a smooth surface, important both for the aesthetics and the aerodynamics. Finally, when most of the work on the vehicle was done, the vehicle was foiled red with 3M Scotchprint.



Figure 4.4: The monocoque with a smooth surface, before being foiled red

4.3 The end product result

The vehicle was revealed to the public on the 22nd of April, where there was quite a bit of media interest for the project and the vehicle (e.g Adressa, Teknisk Ukeblad, e45 and TV2 Nyhetene). Figure 4.5 shows the end result from different angles.

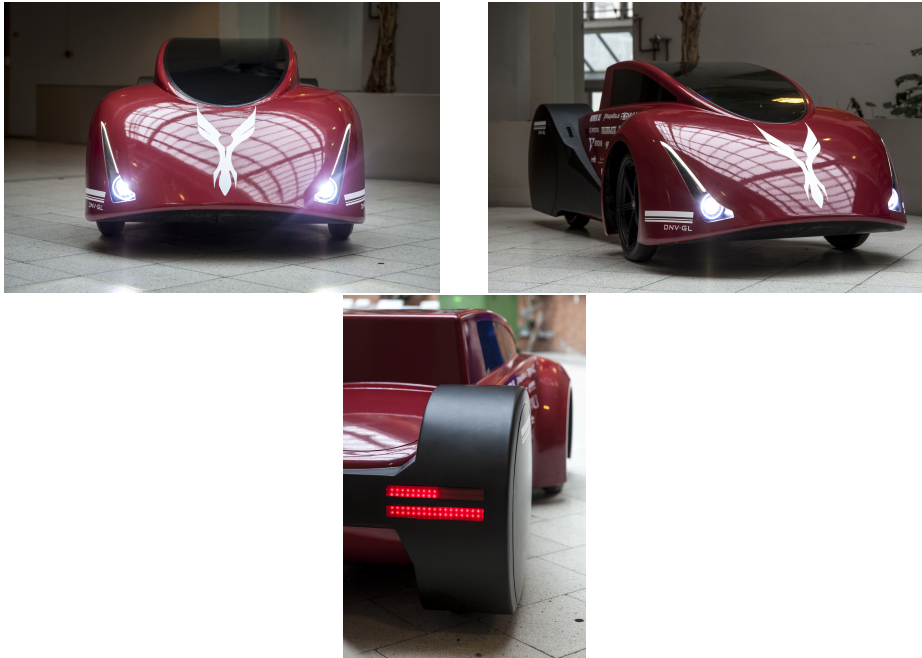


Figure 4.5: Pictures of the end result

In SEM Europe 2015, DNV GL Fuel Fighter was competing in both vehicle classes. The Prototype had a fuel consumption of 483km/kWh, which yielded an 11th place out of 51 contestants in the prototype electric battery class. The new Urban Concept did not get any approved attempt, because of some leakage problems with the fuel cells. Out of 17 teams running on hydrogen fuel cells, only eight teams achieved approved attempts, which might suggest that fuel cells are very difficult to handle. The Urban Concept was however the runner-up for the design award[35]. Overall the team did not completely reach the vision, by not performing on the top level on Shell, but the team managed to create a buzz around the project by having much media attention. The mission of the team was reached by being the runner up for the design award.

Chapter 5

Further work - Advice to next year's team

This year the design approach was not much focusing on the aerodynamic aspect, which is why the cross sectional area is not at its minimum and the vehicle design doesn't have a slender rear end. The ratio of the cross section between the new Urban Concept and smallest cross section limited by SEM rules are in equation 5.1. Where $A_{smallest}$ and A_{urban} are the cross section the smallest cross section limited by SEM and the cross section of the new Urban Concept.

$$\text{cross section ratio} = \frac{A_{smallest}}{A_{urban}} = \frac{12000cm^2}{13065cm^2} = 0.918 \quad (5.1)$$

If it is assumed that the air density, the vehicle's speed and the drag coefficient are the same for both vehicles, the only difference is the cross sectional ratio. This means that the smallest cross sectional ratio would have 91.8 % of the aerodynamic drag of the current cross section. Of course the vehicle's cross section is also affecting the flow and therefore the drag coefficient, but this is just a simplification for giving an idea how much vehicle's cross section is affecting the drag.

Figure 5.1 is showing the streamlines over the new Urban Concept. The rear end of the vehicle has a big wake, and this wake represents much of the pressure drag sources. For further work, a tail could have been developed to on the new Urban Concept, to reduce the drag. Additionally, perhaps the tail could have been re-attachable, to attach the tail during the SEM competition and remove it for the design award. This feature could also be a good design argument.

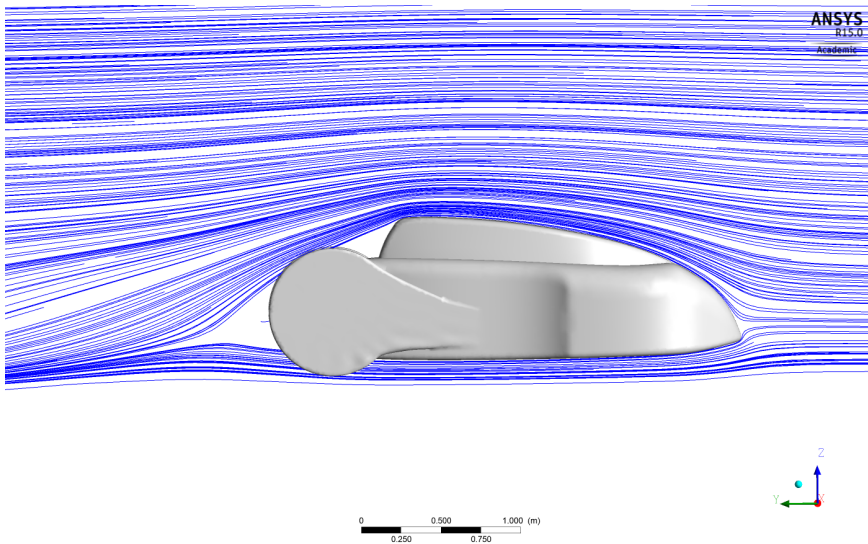


Figure 5.1: The streamline of the new Urban Concept

As explained in chapter 2, vehicle aerodynamic is more than just minimizing the aerodynamic drag. The vehicle's ventilation system for the fuel cell and motor were attached by intuition, and set to each rear end side of the vehicle, and one on the top motor and fuel cells compartment as shown in figure 5.2a and 5.2b, respectively.



(a) At rear side ventilation



(b) At the top compartment ventilation

Figure 5.2: The fuel cells and motor's ventilation system

Other aerodynamic simulation could be finding the aerodynamic interaction with other vehicles. This is not frequently happening in SEM, but occasionally other vehicles have better acceleration (like e.g the combustion engine vs. electrical motor), and therefore interaction may happen. Optimization between aerodynamic

interaction with other vehicles and the motor power lost could be found, to have the ultimate fuel efficient driving cycle. Additionally, analysing the ventilation system and wind noise for the driver may be performed, in order to increase driver comfort. These features have the benefit of also potentially being arguments for design award.

References

- [1] t. t. C. The prototype, “<http://www.cleanmpg.com/forums/showthread.php?t=49763>,” 2013.
- [2] C. P. S. U. a. S. L. O. Prototype, “<http://www.wired.com/2008/03/eco-marathon-08/>,”
- [3] T. prototype, “<http://www.forbescustom.com/EnergyPgs/ShellEcoMarathonP1.html>,”
- [4] L. T. U. Urban Concept, “<http://orgs.latech.edu/ecocar/>,”
- [5] T. U. o. S. Urban Concept, “http://www.avtostrast.eu/?attachment_id=2034,” 2011.
- [6] U. o. S. Urban Concept, “<http://blog.nus.edu.sg/nusid/2009/04/27/design-incubation-centre-launched-latest-eco-friendly-urban-concept-car/>,”
- [7] W.-H. Hucho, ed., *Aerodynamics of Road Vehicles: From Fluid Mechanics to Vehicle Engineering*. Warrendale, PA: Society of Automotive Engineers Inc, 4 edition ed., Feb. 1998.
- [8] R. Barnard, *Road vehicle aerodynamic design: an introduction*. St. Albans, Hertfordshire: Mechaero, 2010.
- [9] “http://www.formula1-dictionary.net/dimpled_surface_finish.html,”
- [10] T. rumpler Limosine figure, “<http://www.carsdiecast.com.au/prod222.htm>,”
- [11] *Shell Eco-Marathon 2015 Official rules chapter 1*. Shell, 2015.
- [12] M. Buodd and B. Halsøy, *Master’s thesis: DNV GL Fuel Fighter towards Shell Eco Maraton 2015*, vol. 2. Jan. 2015.
- [13] N. H. Hossein, *Reliability Systems Engineering For Shell Eco-Marathon Competition*. Jan. 2015.
- [14] O. Bauck, “Master thesis: Hardware and software design for the DNV GL Fuel Fighter vehicles,” June 2015.
- [15] V. Myklebust, “Driver Interface for Shell Eco Marathon Vehicle,” Oct. 2015.

- [16] J. Rief and E. Edwin, “Bachelor thesis: The rear suspension, gear and motor mount for the DNV GL FuelFighter Urban concept car 2015,” May 2015.
- [17] T. S. Center, S. o. A. E. H. T. Committee, U. S. E. Research, and D. Administration, *Tire rolling losses and fuel economy: an R & D Planning Workshop*. Society of Automotive Engineers, 1977.
- [18] J. D. Hunt, J. D. Walter, and G. L. Hall, *The Effect of Tread Polymer Variations on Radial Tire Rolling Resistance*. 1977.
- [19] P. f. s. t. 2, “http://www.thecartech.com/subjects/auto_eng/Road_loads.htm,”
- [20] F. White, *Fluid Mechanics with Student DVD*. New York, N.Y.: McGraw-Hill Science/Engineering/Math, 7 edition ed., Feb. 2010.
- [21] F. Stern, R. V. Wilson, H. W. Coleman, and E. G. Paterson, “Comprehensive Approach to Verification and Validation of CFD Simulations—Part 1: Methodology and Procedures,” *Journal of Fluids Engineering*, vol. 123, pp. 793–802, July 2001.
- [22] *Guide for the Verification and Validation of Computational Fluid Dynamics Simulations (G-077-1998e)*. S.l.: American Institute of Aeronautics & Astronautics, Mar. 1999.
- [23] R. M. Faleide, *Shell Eco Marathon : Electric Drive for World’s Most Fuel Efficient Car*. Institutt for elkraftteknikk, 2009.
- [24] A. B. Espeland, H. Gudvangen, P. T. Larsen, and H. J. Seiness, *Development and Construction of Vehicle for Participation in the Shell Eco-marathon Competition*. Institutt for produktutvikling og materialer, 2012. A team of 13 NTNU students have developed and built a car to compete in the Shell Eco-Marathon 2012 competition. This master project is a continuation of the specialization project done in the aut ...
- [25] R. figure, “Modelled in the rendrings software KeyShot,”
- [26] B. Blocken, T. Stathopoulos, and J. Carmeliet, “CFD simulation of the atmospheric boundary layer: wall function problems,” *Atmospheric Environment*, vol. 41, pp. 238–252, Jan. 2007.
- [27] R. B. Sharma and R. Bansal, “CFD simulation for flow over passenger car using tail plates for aerodynamic drag reduction,” *IOSR Journal of Mechanical and Civil Engineering (IOSR-JMCE)*, vol. 7, no. 5, pp. 28–35, 2013.
- [28] J. Howell and D. Hickman, “The Influence of Ground Simulation on the Aerodynamics of a Simple Car Model,” SAE Technical Paper 970134, SAE International, Warrendale, PA, Feb. 1997.
- [29] D. Mitra, “Design optimization of ground clearance of domestic cars,” *International Journal of Engineering Science and Technology*, vol. 2, no. 7, pp. 2678–2680, 2010.

- [30] D. C. Wilcox, *Turbulence modeling for CFD*. La Cãnada, Calif.: DCW Industries, 1998.
- [31] M. Lanfrit, *Best practice guidelines for handling automotive external aerodynamics with FLUENT*. Version, 2005.
- [32] R. Bhaskaran and L. Collins, “Introduction to CFD basics,” *Cornell University-Sibley School of Mechanical and Aerospace Engineering*, 2002.
- [33] W. H. Hucho, L. J. Janssen, and H. J. Emmelmann, “The Optimization of Body Details-A Method for Reducing the Areodynamic Drag of Road Vehicles,” SAE Technical Paper 760185, SAE International, Warrendale, PA, Feb. 1976.
- [34] R. Barnard, *Road vehicle aerodynamic design: an introduction*. St. Albans, Hertfordshire: Mechaero, 2010.
- [35] S. homepage about the off track award, <http://www.shell.com/global/environment-society/ecomarathon/events/europe/2015-highlights/off-track-award-winners.html>.

Appendix 
The SEM requirements

SEM requirements

Quality	Must	Should
Rigid body	x	
Easy to access compartments	x	
Towing hook	x	
Solid floor	x	
Visibility ahead and 90 degrees to each side	x	
Rear view mirror	x	
Body covering all mechanical parts	x	
Self-made body parts	x	
Four wheels	x	
Non-shattering glass	x	
Mounting of components like battery etc.	x	
Monocoque strong enough protect the driver in a collision or rollover	x	
Roll bar	x	
Safety belt	x	
Emergency shut-down (internal and external)	x	
Brakes	x	
Windscreen	x	
Windscreen wipers	x	
Luggage compartment	x	
Front lights	x	
Front turn indicators	x	
Rear turn indicators	x	
Rear brake light	x	
Rear lights	x	
Fire Extinguisher	x	
Hydrogen detector (for fuel cell)	x	

Appendix **B**
User requirements

Product: Urban Concept	Description	User demands	
		Must	Should
Driver			
Functional			
	Comfortable driving position		x
	Reliable control system (steering, brakes etc.)	x	
	Air-conditioning		x
	Able to follow driving rules	x	
	Satisfying all SEM rules	x	
	Easy to enter and exit	x	
	No fogging on the windows		x
Environmental			
	Operate in both dry and wet weather	x	
	Minimal spill of car liquids (hydraulic oil, battery acid, hydrogen. etc.)		x
	Breathable air inside the cockpit	x	
	Operate on different surfaces	x	
Safety			
	Can exit the car within 10 sec	x	
	Satisfy the SEM rules for driving	x	
	Satisfy the SEM rules for clothing	x	
SEM Rules			
Functional			
	Construct the monocoque according to the SEM rules	x	
	Construct the mechanical parts so the car passes the safety inspection	x	
	Have a design who can win the Design Award	x	
Safety			
	Satisfy the SEM rules for construction	x	
	Satisfy the SEM rules for driving	x	
	Satisfy the SEM rules for clothing	x	
Documentation			
	Deliver the required documentation to SEM	x	

DNV GL Fuel Fighter			
Functional			
	Easy to lift for repairs		x
	Easy access to parts for repairs		x
	Fuel cell	x	
Environmental			
	Able to handle transport (fixing point etc.)	x	
	Can withstand the workshop and people that touches	x	
	Can withstand stand life		x
	Can withstand dust and sand during building	x	
Operational			
	Easy maintenance		x
	Standardized spare parts		x
	Covers are easily removable		x
	Every tools can easy access the part		x
Cost			
	Must not exceed the budget	x	
Safety			
	Follow the NTNU safety requirements when work at NTNU	x	
	Wear safety equipment when it is required	x	
	Follow the SEM safety requirements when work in Rotterdam	x	
Sponsors			
Functional			
	Innovative solutions (DNV GL)	x	
Environmental			
	Give the sponsors their expected publicity	x	
	Have regularly contact with main sponsors		x
Safety			
	Satisfy the expected safety goals	x	

Appendix **C**
**The Buckingham Pi Dimensional
analysis**

$$F = f(L, U, \rho, \mu) \quad (1)$$

List of dimension of each variable

F	L	U	ρ	μ
$\{MLT^{-2}\}$	$\{L\}$	$\{LT^{-1}\}$	$\{ML^{-3}\}$	$\{ML^{-1}T^{-1}\}$

$$n - j = k$$

$$5 - 3 = 2$$

n dimensional variables

k dimensionless variables (exactly two dimensionless group)

j repeating variables (L, U, ρ)

$$\pi_1 = L^a U^b \rho^c F = (L)^a (LT^{-1})^b (ML^{-3})^c (MLT^{-2}) = M^0 L^0 T^0 \quad (2)$$

$$a + b - 3c + 1 = 0 \quad (3)$$

$$c + 1 = 0 \quad (4)$$

$$-b - 2 = 0 \quad (5)$$

$$a = 2, b = -2, c = -1 \quad (6)$$

$$\pi_1 = L^{-2} U^{-2} \rho^{-1} F = \frac{F}{\rho U^2 L^2} = C_F \quad (7)$$

$$\pi_2 = L^a U^b \rho^c \mu^{-1} = (L)^a (LT^{-1})^b (ML^{-3})^c (ML^{-1}T^{-1})^{-1} = M^0 L^0 T^0 \quad (8)$$

$$a + b - 3c + 1 = 0 \quad (9)$$

$$c - 1 = 0 \quad (10)$$

$$-b + 1 = 0 \quad (11)$$

$$a = b = c = 1 \quad (12)$$

$$\pi_2 = L^1 U^1 \rho^1 \mu = \frac{\rho U L}{\mu} = Re \quad (13)$$

$$\frac{F}{\rho U^2 L^2} = g\left(\frac{\rho U L}{\mu}\right) \quad (14)$$

$$C_F = g(Re) \quad (15)$$

By this it can be concluded that the drag and lift coefficient depends on one dimensionless number; Reynolds number. For geometrically similarity the scale model should have the same Reynolds numbers as the real model.

$$\frac{\rho U L}{\mu} = \frac{\rho U_m L_m}{\mu} \quad (16)$$

$$U L = U_m L_m \quad (17)$$

$$U_m = \frac{U L}{L_m} \quad (18)$$

Appendix D

The tyre properties of the Old Urban Concept

MICHELIN TYRES AND RIMS CHARACTERISTICS Urban Concept

TECHNICAL SPECIFICATIONS

Maximum pressure: 500 kPa
 Max pressure for storage: 100 kPa
 Electrical resistance: 5 E+12 Ω
 Load capacity: 100 kg
 Speed limit: 70 km/h

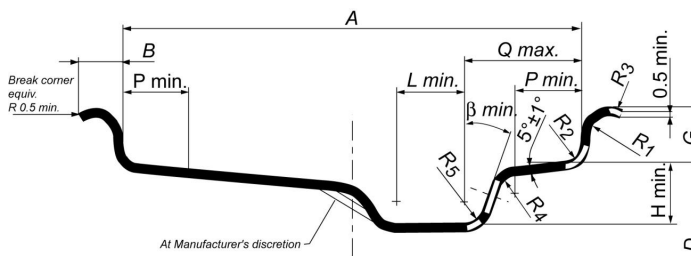
TYRE DIMENSIONS

TYRE SIZE DIMENSION	Section width mm	Overall Diameter mm
95/80 R16	95	558

Theoretical dimensions depending on pressure and rim

RIMS DIMENSIONS

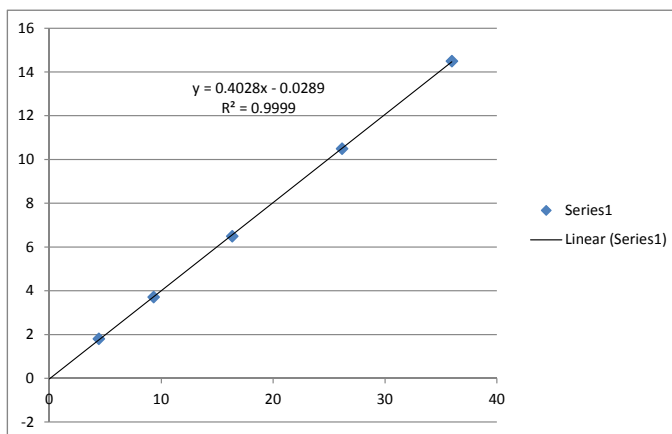
RIM Contour	DIMENSIONS (mm)												
	A		B		G	P	H	L	Q	R1	R2	ββ	D
			min	max	±0,6	min.	min.	min.	max.	min.	max.	min.	
3,00 B	76	±1	10	13	14,1	13	15	16	28	7,5	4,5	10°	405,6
3,50 B	89	±1	10	13	14,1	15	15	19	34	7,5	4,5	13°	405,6



Appendix E

The calibration of the Beam scale

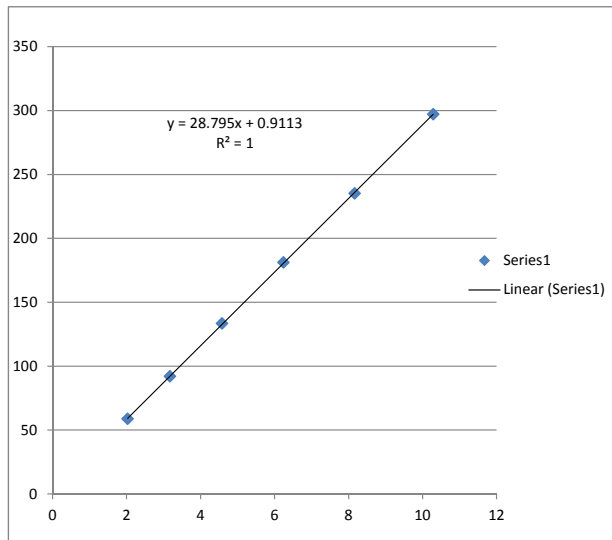
Time	°C	Channel 2 [volt diff]	mass [kg]	force [N]
15:10:05	23.57	5.576144	14.496773	3.6667 35.97033
15:10:35	23.59	1.571933	10.492562	2.667 26.16327
15:11:02	23.5	-2.42548	6.495146	1.667 16.35327
15:11:43	23.63	-5.21158	3.709052	0.95 9.3195
15:12:15	23.62	-7.11408	1.806554	0.45 4.4145
15:12:34	23.62	-8.92063	0	0 0



Appendix F

The calibration of the Pitot tube

Time	degree [°C]	Channel 1 [V]	StdDev 1	mm alc	delta p	volt diff
14:15:52	23.7	-9.100534	0.003171		0	
14:20:20	23.84	1.185893	0.169578	187	297.1841	10.28643
14:21:46	23.87	-0.935227	0.125431	148	235.2046	8.165307
14:23:37	23.95	-2.862987	0.097654	114	181.1711	6.237547
14:26:20	23.84	-4.520452	0.078975	84	133.4945	4.580082
14:28:00	23.86	-5.927027	0.047193	58	92.17476	3.173507
14:30:22	23.81	-7.072992	0.025498	37	58.80114	2.027542




```

(left-button-function mouse-rotate)
(hidden-surfaces? #t)
(axes/visible? #t)
(cx-case-version (15 0 0))
))
(bc (air fluid mixture) (
(material . air)
(sources? . #f)
(source-terms)
(fixed? . #f)
(cylindrical-fixed-var? . #f)
(fixes)
(mrf-motion? . #f)
(mrf-relative-to-thread . -1)
(mrf-omega (constant . 0) (profile "" ""))
(mrf-grid-x-vel (constant . 0) (profile "" ""))
(mrf-grid-y-vel (constant . 0) (profile "" ""))
(mrf-grid-z-vel (constant . 0) (profile "" ""))
(mrf-x-origin (constant . 0) (profile "" ""))
(mrf-y-origin (constant . 0) (profile "" ""))
(mrf-z-origin (constant . 0) (profile "" ""))
(mrf-ai (constant . 0) (profile "" ""))
(mrf-aj (constant . 0) (profile "" ""))
(mrf-ak (constant . 1) (profile "" ""))
(mrf-udf-zmotion-name . "none")
(mgrid-motion? . #f)
(mgrid-relative-to-thread . -1)
(mgrid-omega (constant . 0) (profile "" ""))
(mgrid-grid-x-vel (constant . 0) (profile "" ""))
(mgrid-grid-y-vel (constant . 0) (profile "" ""))
(mgrid-grid-z-vel (constant . 0) (profile "" ""))
(mgrid-x-origin (constant . 0) (profile "" ""))
(mgrid-y-origin (constant . 0) (profile "" ""))
(mgrid-z-origin (constant . 0) (profile "" ""))
(mgrid-ai (constant . 0) (profile "" ""))
(mgrid-aj (constant . 0) (profile "" ""))
(mgrid-ak (constant . 1) (profile "" ""))
(mgrid-udf-zmotion-name . "none")
(deactivated? . #f)
(les-embedded-spec . 0)
(les-embedded-mom-scheme . 0)

```

```

(les-embedded-c-wale . 0.325)
(les-embedded-c-smag . 0.1)
(porous? . #f)
(conical? . #f)
(direction-1/x (constant . 1) (profile "" ""))
(direction-1/y (constant . 0) (profile "" ""))
(direction-1/z (constant . 0) (profile "" ""))
(direction-2/x (constant . 0) (profile "" ""))
(direction-2/y (constant . 1) (profile "" ""))
(direction-2/z (constant . 0) (profile "" ""))
(cone-axis/x . 1)
(cone-axis/y . 0)
(cone-axis/z . 0)
(cone-axis-pt/x . 1.)
(cone-axis-pt/y . 0)
(cone-axis-pt/z . 0)
(cone-angle . 0)
(rel-vel-resistance? . #t)
(porous-r/1 (constant . 0) (profile "" ""))
(porous-r/2 (constant . 0) (profile "" ""))
(porous-r/3 (constant . 0) (profile "" ""))
(alt-inertial-form? . #f)
(porous-c/1 (constant . 0) (profile "" ""))
(porous-c/2 (constant . 0) (profile "" ""))
(porous-c/3 (constant . 0) (profile "" ""))
(c0 . 0)
(c1 . 0)
(porosity (constant . 1) (profile "" ""))
(area-density (constant . 1) (profile "" ""))
(heat-transfer-coeff (constant . 1) (profile "" ""))
))
(bc (interior-air interior mixture) (
))
(bc (ahmed-body wall mixture) (
(planar-conduction? . #f)
(motion-bc . 0)
(shear-bc . 0)
(relative? . #t)
(rotating? . #f)
(vmag . 0)
(ni . 1)

```

```

(nj . 0)
(nk . 0)
(components? . #f)
(u (constant . 0) (profile "" ""))
(v (constant . 0) (profile "" ""))
(w (constant . 0) (profile "" ""))
(omega . 0)
(x-origin . 0)
(y-origin . 0)
(z-origin . 0)
(ai . 0)
(aj . 0)
(ak . 1)
(shear-x (constant . 0) (profile "" ""))
(shear-y (constant . 0) (profile "" ""))
(shear-z (constant . 0) (profile "" ""))
(fslip . 0)
(eslip . 0)
(specular-coeff . 0)
(thermal-stabilization? . #f)
(scale-factor . 0)
(stab-method . 1)
))
(bc (velocity-inlet velocity-inlet mixture) (
(velocity-spec . 2)
(frame-of-reference . 0)
(vmag (constant . 0) (profile "" ""))
(p_sup (constant . 0) (profile "" ""))
(coordinate-system . 0)
(u (constant . 0) (profile "" ""))
(v (constant . 0) (profile "" ""))
(w (constant . 0) (profile "" ""))
(ni (constant . 1) (profile "" ""))
(nj (constant . 0) (profile "" ""))
(nk (constant . 0) (profile "" ""))
(ai . 1)
(aj . 0)
(ak . 0)
(x-origin . 0)
(y-origin . 0)
(z-origin . 0)

```

```

(omega-swirl . 0)
(mixing-plane-thread? . #f)
))
(bc (pressure-outlet pressure-outlet mixture) (
(p (constant . 0) (profile "" ""))
(direction-spec . 1)
(coordinate-system . 0)
(ni (constant . 1) (profile "" ""))
(nj (constant . 0) (profile "" ""))
(nk (constant . 0) (profile "" ""))
(ai . 1)
(aj . 0)
(ak . 0)
(x-origin . 0)
(y-origin . 0)
(z-origin . 0)
(mixing-plane-thread? . #f)
(radial? . #f)
(avg-press-spec? . #f)
(avg-option . 0)
(targeted-mf-boundary? . #f)
(targeted-mf (constant . 1) (profile "" ""))
(targeted-mf-pmax (constant . 5000000.) (profile "" ""))
(targeted-mf-pmin (constant . 1) (profile "" ""))
))
(bc (road wall mixture) (
(planar-conduction? . #f)
(motion-bc . 0)
(shear-bc . 0)
(relative? . #t)
(rotating? . #f)
(vmag . 0)
(ni . 1)
(nj . 0)
(nk . 0)
(components? . #f)
(u (constant . 0) (profile "" ""))
(v (constant . 0) (profile "" ""))
(w (constant . 0) (profile "" ""))
(omega . 0)
(x-origin . 0)

```

```

(y-origin . 0)
(z-origin . 0)
(ai . 0)
(aj . 0)
(ak . 1)
(shear-x (constant . 0) (profile "" ""))
(shear-y (constant . 0) (profile "" ""))
(shear-z (constant . 0) (profile "" ""))
(fslip . 0)
(eslip . 0)
(specular-coeff . 0)
(thermal-stabilization? . #f)
(scale-factor . 0)
(stab-method . 1)
))
(bc (symmetry symmetry mixture) (
))
(bc (no-shear_boundary wall mixture) (
(planar-conduction? . #f)
(motion-bc . 0)
(shear-bc . 0)
(relative? . #t)
(rotating? . #f)
(vmag . 0)
(ni . 1)
(nj . 0)
(nk . 0)
(components? . #f)
(u (constant . 0) (profile "" ""))
(v (constant . 0) (profile "" ""))
(w (constant . 0) (profile "" ""))
(omega . 0)
(x-origin . 0)
(y-origin . 0)
(z-origin . 0)
(ai . 0)
(aj . 0)
(ak . 1)
(shear-x (constant . 0) (profile "" ""))
(shear-y (constant . 0) (profile "" ""))
(shear-z (constant . 0) (profile "" ""))

```

```
(fslip . 0)
(eslip . 0)
(specular-coeff . 0)
(thermal-stabilization? . #f)
(scale-factor . 0)
(stab-method . 1)
))
(ni ((2 air)(1 interior-air)(5 ahmed-body)(6 velocity-inlet)(7 pressure-
```


Appendix **H**

Urban Concept 2 Fluent set up script

```
(rp (
(strategy/solution-strategy/modifications ((type . list-class) (min-length 1)))
(strategy/solution-strategy/original-settings ((type . struct-class) (min-length 1)))
(strategy/solution-strategy/before-init-modification ((type . struct-class) (min-length 1)))
(strategy/initialization-strategy ((selection . init-from-case) (type . list-class) (min-length 1)))
(domains (((1 geom-domain mixture) (children) (material . air))))
(monitor/lift ((cl-1 (cl-file . #f) (data? . #t) (thread-list 5) (per-zone 1)))
(monitor/drag ((cd-1 (cd-file . #f) (data? . #t) (thread-list 5) (per-zone 1)))
(autosave/run-number 1)
(epsilon/default 0.009751752018928528)
(k/default 0.003978373948484659)
(turb-viscosity/relax 0.800000011920929)
(flow/scheme 24)
(hyb-init/variables (((domain-id . 1) (zone-type . 0) (solution-zones 2)))
(species/isat-file "Z:\07 - Personal Folders\myselie\Aero1\test3_files\dynamesh\isat.dat")
(pressure/flow-init-type 1)
(pressure-coupled/pressure/explicit-relax 0.25)
(pressure-coupled/mom/explicit-relax 0.25)
(pressure-coupled/courant-number 50.)
(pressure/scheme 10)
(y-velocity/default 5.149999618530273)
(mom/scheme 0)
(residuals/window 0)
(mesh/interpolate-in-time? #f)
(mesh/grid-check-performed? #t)
(dynamesh/motion-history/basename "Z:\07 - Personal Folders\myselie\Aero1\test3_files\dynamesh\motion-history")
(dynamesh/in-cyn/crank-period 10000000000.)
(dynamesh/in-cyn/crank-rpm 0.16666666666666667)
(dynamesh/remesh/repartition-interface-threshold 10.)
```

```

(dynamesh/remesh/repartition-interval 10)
(number-of-iterations 100)
(materials ((air fluid (chemical-formula . #f) (density (constant . 1.225)
(parallel/separate-and-order 0)
(case-config ((rp-seg? . #t) (rp-acoustics? . #f) (rp-atm? . #f) (rp-axi?
(reference-viscosity 1.789400084817316e-05)
(reference-velocity 5.149999618530273)
(reference-density 1.225000023841858)
(reference-area 0.478512704372406)
(des-sa-on? #f)
(ke-realizability-on? #t)
(ke-non-eqm #t)
(ke-std-wall? #f)
(cfd-post-mesh-info ((0 0 (air) (car wall air) (road wall air) (symmetry
))
(dv (
))
(cx (
(gui-processing? #t)
(surfaces/groups ((inlet (0)) (outlet (1)) (wall (2)) (symmetry (3)) (road
(cx-virtual-id-list (4196 4197 4198 4199 4200 4201 4202))
(cx-surface-id-map ((6 4202) (5 4201) (4 4200) (3 4199) (2 4198) (1 4197)
(cx-surface-type ((0 0) (1 0) (2 0) (3 0) (4 0) (5 0) (6 0)))
(cx-surface-def-list ((4202 () (zone-surface 4202 1) #f) (4201 () (zone-s
(cx-surface-list #((0 ((zid 10) (type zone-surf) (name inlet) (status sus
(view-list ((front ((0.796567572713087 6.011897563934326 76.8417989775152
(left-button-function mouse-rotate)
(render/surfaces (0 1 2 3 4 5))
(render/grid/surfaces (0 1 2 3 4 5))
(hidden-surfaces? #t)
(axes/visible? #t)
(cx-case-version (15 0 0))
))
(bc (air fluid mixture) (
(material . air)
(sources? . #f)
(source-terms)
(fixed? . #f)
(cylindrical-fixed-var? . #f)
(fixes)
(mrf-motion? . #f)

```

```

(mrf-relative-to-thread . -1)
(mrf-omega (constant . 0) (profile "" ""))
(mrf-grid-x-vel (constant . 0) (profile "" ""))
(mrf-grid-y-vel (constant . 0) (profile "" ""))
(mrf-grid-z-vel (constant . 0) (profile "" ""))
(mrf-x-origin (constant . 0) (profile "" ""))
(mrf-y-origin (constant . 0) (profile "" ""))
(mrf-z-origin (constant . 0) (profile "" ""))
(mrf-ai (constant . 0) (profile "" ""))
(mrf-aj (constant . 0) (profile "" ""))
(mrf-ak (constant . 1) (profile "" ""))
(mrf-udf-zmotion-name . "none")
(mgrid-motion? . #f)
(mgrid-relative-to-thread . -1)
(mgrid-omega (constant . 0) (profile "" ""))
(mgrid-grid-x-vel (constant . 0) (profile "" ""))
(mgrid-grid-y-vel (constant . 0) (profile "" ""))
(mgrid-grid-z-vel (constant . 0) (profile "" ""))
(mgrid-x-origin (constant . 0) (profile "" ""))
(mgrid-y-origin (constant . 0) (profile "" ""))
(mgrid-z-origin (constant . 0) (profile "" ""))
(mgrid-ai (constant . 0) (profile "" ""))
(mgrid-aj (constant . 0) (profile "" ""))
(mgrid-ak (constant . 1) (profile "" ""))
(mgrid-udf-zmotion-name . "none")
(deactivated? . #f)
(laminar? . #f)
(laminar-mut-zero? . #t)
(les-embedded-spec . 0)
(les-embedded-mom-scheme . 0)
(les-embedded-c-wale . 0.325)
(les-embedded-c-smag . 0.1)
(porous? . #f)
(conical? . #f)
(direction-1/x (constant . 1) (profile "" ""))
(direction-1/y (constant . 0) (profile "" ""))
(direction-1/z (constant . 0) (profile "" ""))
(direction-2/x (constant . 0) (profile "" ""))
(direction-2/y (constant . 1) (profile "" ""))
(direction-2/z (constant . 0) (profile "" ""))
(cone-axis/x . 1)

```

```

(cone-axis/y . 0)
(cone-axis/z . 0)
(cone-axis-pt/x . 1.)
(cone-axis-pt/y . 0)
(cone-axis-pt/z . 0)
(cone-angle . 0)
(rel-vel-resistance? . #t)
(porous-r/1 (constant . 0) (profile "" ""))
(porous-r/2 (constant . 0) (profile "" ""))
(porous-r/3 (constant . 0) (profile "" ""))
(alt-inertial-form? . #f)
(porous-c/1 (constant . 0) (profile "" ""))
(porous-c/2 (constant . 0) (profile "" ""))
(porous-c/3 (constant . 0) (profile "" ""))
(c0 . 0)
(c1 . 0)
(porosity (constant . 1) (profile "" ""))
(area-density (constant . 1) (profile "" ""))
(heat-transfer-coeff (constant . 1) (profile "" ""))
))
(bc (interior-air interior mixture) (
))
(bc (car wall mixture) (
(planar-conduction? . #f)
(motion-bc . 0)
(shear-bc . 0)
(relative? . #t)
(rotating? . #f)
(vmag . 0)
(ni . 1)
(nj . 0)
(nk . 0)
(components? . #f)
(u (constant . 0) (profile "" ""))
(v (constant . 0) (profile "" ""))
(w (constant . 0) (profile "" ""))
(roughness-height (constant . 0) (profile "" ""))
(roughness-const (constant . 0.5) (profile "" ""))
(omega . 0)
(x-origin . 0)
(y-origin . 0)

```

```

(z-origin . 0)
(ai . 0)
(aj . 0)
(ak . 1)
(shear-x (constant . 0) (profile "" ""))
(shear-y (constant . 0) (profile "" ""))
(shear-z (constant . 0) (profile "" ""))
(fslip . 0)
(eslip . 0)
(specular-coeff . 0)
(thermal-stabilization? . #f)
(scale-factor . 0)
(stab-method . 1)
))
(bc (road wall mixture) (
(planar-conduction? . #f)
(motion-bc . 0)
(shear-bc . 0)
(relative? . #t)
(rotating? . #f)
(vmag . 0)
(ni . 1)
(nj . 0)
(nk . 0)
(components? . #f)
(u (constant . 0) (profile "" ""))
(v (constant . 0) (profile "" ""))
(w (constant . 0) (profile "" ""))
(roughness-height (constant . 0) (profile "" ""))
(roughness-const (constant . 0.5) (profile "" ""))
(omega . 0)
(x-origin . 0)
(y-origin . 0)
(z-origin . 0)
(ai . 0)
(aj . 0)
(ak . 1)
(shear-x (constant . 0) (profile "" ""))
(shear-y (constant . 0) (profile "" ""))
(shear-z (constant . 0) (profile "" ""))
(fslip . 0)

```

```

(eslip . 0)
(specular-coeff . 0)
(thermal-stabilization? . #f)
(scale-factor . 0)
(stab-method . 1)
))
(bc (symmetry symmetry mixture) (
))
(bc (wall wall mixture) (
(planar-conduction? . #f)
(motion-bc . 0)
(shear-bc . 1)
(relative? . #t)
(rotating? . #f)
(vmag . 0.)
(ni . 1.)
(nj . 0.)
(nk . 0.)
(components? . #f)
(u (constant . 0.) (profile "" ""))
(v (constant . 0.) (profile "" ""))
(w (constant . 0.) (profile "" ""))
(roughness-height (constant . 0.) (profile "" ""))
(roughness-const (constant . 0.5) (profile "" ""))
(omega . 0.)
(x-origin . 0.)
(y-origin . 0.)
(z-origin . 0.)
(ai . 0.)
(aj . 0.)
(ak . 1.)
(shear-x (constant . 0.) (profile "" ""))
(shear-y (constant . 0.) (profile "" ""))
(shear-z (constant . 0.) (profile "" ""))
(fslip . 0.)
(eslip . 0.)
(specular-coeff . 0.)
(thermal-stabilization? . #f)
(scale-factor . 0.)
(stab-method . 1)
))

```

```

(bc (outlet pressure-outlet mixture) (
(p (constant . 0) (profile "" ""))
(direction-spec . 1)
(coordinate-system . 0)
(ni (constant . 1) (profile "" ""))
(nj (constant . 0) (profile "" ""))
(nk (constant . 0) (profile "" ""))
(ai . 1)
(aj . 0)
(ak . 0)
(x-origin . 0)
(y-origin . 0)
(z-origin . 0)
(ke-spec . 2)
(k (constant . 1) (profile "" ""))
(e (constant . 1) (profile "" ""))
(turb-intensity . 0.05)
(turb-length-scale . 1)
(turb-hydraulic-diam . 1)
(turb-viscosity-ratio . 10)
(mixing-plane-thread? . #f)
(radial? . #f)
(avg-press-spec? . #f)
(avg-option . 0)
(targeted-mf-boundary? . #f)
(targeted-mf (constant . 1) (profile "" ""))
(targeted-mf-pmax (constant . 5000000.) (profile "" ""))
(targeted-mf-pmin (constant . 1) (profile "" ""))
))
(bc (inlet velocity-inlet mixture) (
(velocity-spec . 2)
(frame-of-reference . 0)
(vmag (constant . 5.15) (profile "" ""))
(p_sup (constant . 0.) (profile "" ""))
(coordinate-system . 0)
(u (constant . 0.) (profile "" ""))
(v (constant . 0.) (profile "" ""))
(w (constant . 0.) (profile "" ""))
(ni (constant . 1.) (profile "" ""))
(nj (constant . 0.) (profile "" ""))
(nk (constant . 0.) (profile "" ""))

```

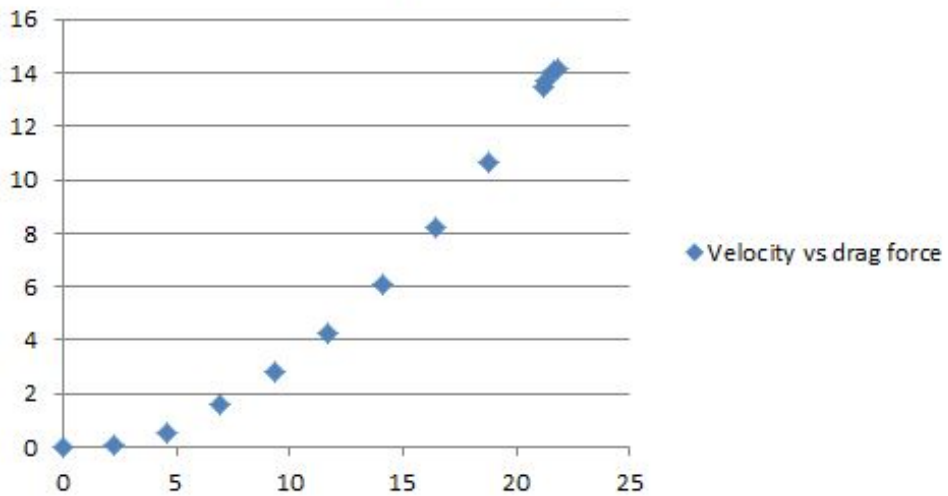
```
(ai . 1.)
(aj . 0.)
(ak . 0.)
(x-origin . 0.)
(y-origin . 0.)
(z-origin . 0.)
(omega-swirl . 0.)
(ke-spec . 2)
(k (constant . 1.) (profile "" ""))
(e (constant . 1.) (profile "" ""))
(turb-intensity . 0.009999999776482582)
(turb-length-scale . 1.)
(turb-hydraulic-diam . 1.)
(turb-viscosity-ratio . 10.)
(mixing-plane-thread? . #f)
))
(ni ((2 air)(1 interior-air)(5 car)(6 road)(7 symmetry)(8 wall)(9 outlet))
```


Appendix I

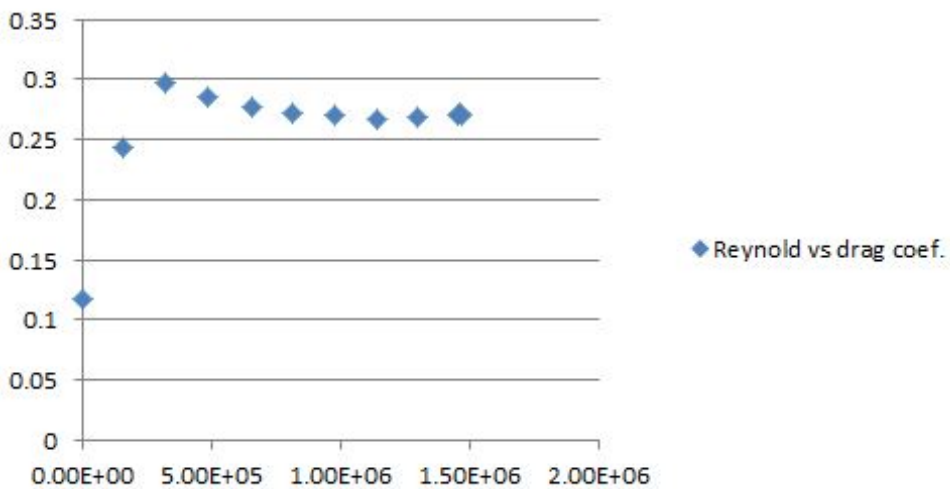
The wind tunnel data results

Ref value	0	22.049	1.20661763	-9.6541	0	0	0	0.00E+00	-9.6391	0	0
100	21.894	1.20725153	-9.5491	0.105	3.023475	2.238048	1.56E+05	-9.6129	0.0262	0.006691	0.117713
200	21.969	1.20719015	-9.2216	0.4325	12.4538375	4.542331	3.17E+05	-9.4154	0.2237	0.571285	0.244001
300	21.922	1.20713697	-8.6435	1.0106	29.100227	6.943603	4.85E+05	-9.0041	0.635	1.621663	0.266419
400	22.122	1.20631932	-7.8205	1.8336	52.798512	9.356097	6.52E+05	-8.5291	1.11	2.834718	0.285582
500	22.494	1.20480145	-6.7887	2.8654	82.509193	11.7033	8.15E+05	-7.956	1.6831	4.298301	0.2771
600	23.04	1.2025805	-5.5097	4.1444	119.337998	14.08793	9.79E+05	-7.2507	2.3884	6.099496	0.271868
700	23.859	1.1992644	-4.0105	5.6436	162.507462	16.46244	1.14E+06	-6.4108	3.2283	8.244433	0.268954
800	25.212	1.1982602	-2.3179	7.3362	211.245979	18.81216	1.30E+06	-5.4769	4.1622	10.02943	0.267648
900	26.899	1.18711384	-0.3933	9.2608	266.664736	21.19589	1.45E+06	-4.3817	5.2574	13.42833	0.267815
910	27.868	1.18329243	-0.3285	9.3156	268.242702	21.29281	1.46E+06	-4.2867	5.3524	13.66896	0.27105
920	29.373	1.17740575	-0.0978	9.5563	275.1736585	21.61998	1.47E+06	-4.138	5.5011	14.04871	0.271564
930	30.079	1.17466443	0.0315	9.6856	278.896852	21.79114	1.48E+06	-4.0905	5.5486	14.17001	0.270252
0	26.122		-9.658					-9.5863			
Ideal gas constant	286.9										
Hg density	13594	kg/m ³									
Gravity	9.81	m/s ²									
Amb. Pressure	766.3	mmHg									
Pitot tube calibration	28.795										
Balance calibration	2.5538										
Characteristic length	1	m									
RPM	Temp	Air density	Pitot tube	pressure diff	Pressure diff	Velocity	Reynolds	balance voltage	balance diff	force	drag
	C	kg/m ³	V	V	Pa	m/s		V		Newton	coef.

Velocity vs drag force
















Reynold vs drag coef.



Appendix J

The morphology table

Material for <u>monocoque</u>	 Carbon Fiber	 Steel	 Aluminum	 Wood	 Cardboard
Rims	 Carbon Fiber	 Steel	 Aluminum	 Wood	
Energy source	 Battery	 Hydrogen	 Shell FuelSave Diesel	 Shell FuelSave Unleaded 95	 Ethanol E100
Motor	 Electrical	 Diesel	 Gasoline		
Suspension	 Carbon Fiber	 Aluminum			
Steering	 Wire	 Go-kart	 Steering box	 Rack & Pinion	 Worm gear